SEED FINAL REPORT

Assessment of Historic Concrete and Masonry by Broadband Vibration Testing

SERDP SEED Project RC-1653

August 2010

Thomas E. Boothby, Ph.D.
Sezer Atamturktur, Ph.D.
Paul Kremer
Elisabetta Pistone
Nicole Trujillo

Penn State University

Strategic Environmental Research and Development Program

REPORT DOCUMENTATION PAGE

Form Approved
OMB No. 0704-0188

PLEASE DO NOT RETURN YOUR FORM TO THE ABOVE ORGANIZATION.

1. REPORT DATE *(DD-MM-YYYY)*	2. REPORT TYPE	3. DATES COVERED *(From - To)*
30-06-2010	SEED Report	28-08-2008 to 30-06-2010

4. TITLE AND SUBTITLE

Assessment of Historic Concrete and Masonry by Broadband Vibration Testing

5a. CONTRACT NUMBER

W912HQ-08-P-0078

5b. GRANT NUMBER

5c. PROGRAM ELEMENT NUMBER

6. AUTHOR(S)

Thomas E. Boothby
Paul Kremer
Elisabetta Pistone
Sezer Atamturktur
Nicole Trujilo

5d. PROJECT NUMBER

5e. TASK NUMBER

5f. WORK UNIT NUMBER

7. PERFORMING ORGANIZATION NAME(S) AND ADDRESS(ES)

Penn State University; Department of Architectural Engineering
104 Engineering Unit A
University Park, PA 16802

8. PERFORMING ORGANIZATION REPORT NUMBER

9. SPONSORING/MONITORING AGENCY NAME(S) AND ADDRESS(ES)

Sustainable Infrastructure Program
SERDP/ESTCP
901 N. Stuart St., Suite 303
Arlington, VA 22203-1853

10. SPONSOR/MONITOR'S ACRONYM(S)

11. SPONSOR/MONITOR'S REPORT NUMBER(S)

12. DISTRIBUTION/AVAILABILITY STATEMENT

Approved for public release; distribution is unlimited

13. SUPPLEMENTARY NOTES

14. ABSTRACT

The assessment of historic concrete and masonry requires a number of diagnostic tests that involve a low-energy impact of the structure and the acquisition and processing of the resulting vibration signals from the structure. This project involved the determination of methods suitable for automation and combination, and the prototyping of these methods in a pair of historic buildings on a DOD installation. The objectives of the project were to test the merit of structural investigations using the air-coupled impact-echo method, which relies on microphones rather than contact devices to obtain diagnostic information, and to determine the suitability of this method for automation and integration with the experimental modal analysis method. The project also included the development of a prototype automated impactor using compressed air-driven hardened steel balls of various diameters. It was found that the air-coupled method was effective in discriminating flaws in masonry and concrete. It was further found that this method can be developed into an automated scanning method for horizontal and vertical surfaces.

15. SUBJECT TERMS

Historic Structures, non-destructive evaluation, impact-echo, experimental modal analysis, concrete, masonry

16. SECURITY CLASSIFICATION OF:			17. LIMITATION OF ABSTRACT	18. NUMBER OF PAGES	19a. NAME OF RESPONSIBLE PERSON
a. REPORT	b. ABSTRACT	c. THIS PAGE	SAR	49	Thomas E. Boothby
					19b. TELEPHONE NUMBER *(Include area code)* (814) 863-2082

Table of Contents

List of Tables

List of Figures

List of Acronyms

AC	Alternating current
ACIE	Air-coupled Imact-Echo
AC/DC	Alternating Current/Direct Current
AFB	Air Force Base
ASTM	American Society for Testing and Materials
DC	Direct Current
DOD	Department of Defense
EMA	Experimental Modal Analysis
HAER	Historic American Engineering Record
IE	Impact-echo
IEPE	Integrated Electronics Piezo Electric (accelerometer)
IEI	Impact Echo Instruments, LLC
I/O	Input/Output
LSCE	Least Squares Complex Exponential
NI	National Instruments
OS	Operating System
PCB	PCB Piezotronics, Inc.
USB	Universal Serial Bus
WPAFB	Wright-Patterson Air Force Base

Keywords

Historic, Concrete, Masonry, Condition Evaluation, Structure, Assessment, Impact-echo, Modal Analysis

Acknowledgements

The authors acknowledge the assistance they received from the staff of the Environmental Management Division and the Base Civil Engineer at Wright-Patterson AFB. The authors particularly acknowledge the contribution of Paul Woodruff, Cultural Resources Program Manager. The authors also thank Kristen Lau, Carrie Wood, and John Hall of the SERDP program for their assistance with the management of this project, and further thank John Hall for his thoughtful review of the initial draft.

Abstract

The objective of this project is to develop a system to assess the structural integrity of concrete and masonry structures, using a combination of the air coupled impact echo method and the experimental modal analysis method to complete a comprehensive assessment of concrete and masonry structures. Specifically, the project was intended to prove that the air-coupled impact-echo method is an effective means of determining the presence of local defects in a concrete or masonry structure. Moreover, it was desirable to show that the air-coupled impact-echo method can be rapidly deployed and operated, and eventually can be automated. It was further considered that the air-coupled impact-echo method could be effectively combined with experimental modal analysis for use as an assessment tool.

The air-coupled impact-echo method was compared to two other impact echo procedures on a floor slabs, concrete columns, and masonry walls. The air-coupled impact-echo method was used effectively to determine the size and depth of defects in concrete and masonry, and to determine individual construction features in masonry walls. The method is simpler to apply because the microphone enclosure used in the air-coupled method can be easily relocated. Based on the construction of an automated impactor, it has been shown that the method is capable of automation. Furthermore, the ease with which experimental modal analysis results can be obtained, and the compatibility of the software and procedures in experimental modal analysis and air-coupled impact echo show that it will be possible to combine the methods into a comprehensive assessment tool.

Objective

The objective of this project is to develop a non-invasive, non-destructive system to assess the structural integrity of historic concrete and masonry structures, using a combination of the air coupled impact echo method and the experimental modal analysis method. These methods will be deployed to complete a comprehensive assessment of concrete and masonry structures. The working hypotheses that support the development of the system are:

1. The air-coupled impact-echo method is an effective means of determining the presence of local defects in a concrete or masonry structure.

2. The air-coupled impact-echo method can be rapidly deployed and operated, and eventually can be automated.

3. The experimental modal analysis (EMA) method, proven in the scientific literature to be an effective means of completing a global assessment of an existing structure, can be effectively combined with the air-coupled impact-echo (ACIE) method to form an efficient means of conducting overall assessments of a concrete or masonry structure.

The risks in this concept are reduced by a series of experiments on concrete and masonry structures that show that the two proposed methods (ACIE and EMA) can be quickly and easily applied in the field to a historic structure. Initial automation efforts will also demonstrate that this is a system that is amenable to automation for rapid implementation and application.

The criteria for success of the present project are:

Demonstrate the effectiveness of the air-coupled impact echo method as a diagnostic tool for walls, floors, and columns. This requires that the method be used in the laboratory and in the field for the determination of commonly occurring defects in concrete and masonry, and for the determination of the construction of these elements.

Demonstrate that the air-coupled impact-echo method is automatable in terms of impact delivery, data acquisition system activation, data collection, and data display. This criterion requires the development of an impactor that is capable of being operated rapidly and is capable of triggering a data acquisition routine. The initial development of the computer programs for this exercise will also assist in the achievement of this success criterion.

Demonstrate that the impact-echo method can be integrated with the experimental modal analysis method in an effective way for determination of local defects and global behavior of a wall or floor. This requires that the impacts used in impact-echo assessment can trigger the data acquisition channels used for experimental modal analysis and that they produce frequency input that can be used in the development of frequency respsonse functions for EMA assessment. This will also require that compatible or fully integrated computer software be deployed for conducting both impact-echo and experimental modal analysis.

Background

The historic concrete and masonry buildings owned by the Department of Defense (DOD) include a wide variety of building types and uses. Frequently recurring types of buildings include brick bearing wall buildings, generally constructed before the 1940's, reinforced concrete frame buildings, which first appear around 1920, and reinforced concrete or steel frames infilled with concrete masonry units, which generally appear after the 1940's. The interior frames of these buildings may be reinforced concrete, steel, or wood. The uses of these buildings are equally varied. They may be used for administrative buildings, residential facilities, hospitals, testing laboratories, power plants, air operations buildings, and others. The challenges in maintaining these structures relate to the integrity of the original construction, to the capacity of the original construction to resist modern code-imposed loading, or to loadings resulting from changed building use.

The determination of the capacity of a building structure requires two separate assessments. The first is a determination of the construction, materials and reinforcement, coupled with an estimate of the structural capacity of the assembly in question. This is generally done by consulting as-built plans, if available, determining the geometry of the structure, estimating the loads on the structure based on modern building codes and standards or based on DOD standards for conducting such assessments. Permissible stresses or levels of internal forces are likewise prescribed by building codes and standards. In general this simplest method is undertaken first, and the more advanced methods are saved for the cases where the structure would be found inadequate by a simple, conservative method.

A second type of assessment involves the determination of the condition of the materials in place. In particular, for concrete and masonry, the assessment must identify whether the concrete has internal defects such as voids, delaminations, or inclusions or whether the strength of the concrete is compromised in some other fashion. Where defects are found, it is necessary to determine whether they have a critical influence on the load-carrying capacity of the structure. This is accomplished at least in part by the structural assessment of the building. As a result, the structural and the materials assessments can be seen as complementary: a materials defect may not be harmful to the building if it is sufficiently small or if it is located within a non-critical area of the structure. During a materials survey for assessment purposes, both of these requirements must be recognized. As complete a picture as possible of the characteristics of the materials in place must be found, and this needs to be tied into the overall structural assessment of the building to make a determination of the damage that can result from the condition of the material.

The principal defects in concrete structures are:

Slabs:
- Delamination—separation of the concrete cover over the top layer of reinforcement
- Voids
- Reinforcement corrosion

Beams:
- Voids
- Areas of segregation (in concrete placed without proper controls, the cement paste becomes separated from the coarse aggregate, resulting in internal rock pockets, surface honeycombing, or other areas of segregation).
- Cracking: structural
- Cracking: thermal, freeze-thaw, environmental
- Reinforcement corrosion

Columns:
- Segregation
- cracking

Walls:
- Segregation
- Cold joints
- Environmental damage
- Reinforcement corrosion

The principal defects in masonry structures are:

Brick masonry (load bearing):
- Lack of bond between wythes
- cracking
- environmental deterioration of masonry units.

Brick masonry (veneer):
- Most problems visible to inspection

Concrete masonry:
- Cracks
- General deterioration
- Reinforcement anchorage

Assessment Methods for Concrete and Masonry Structures

A number of assessment methods have been proposed or implemented for the diagnosis of problems in concrete and masonry. These methods may be destructive, involving the removal of material from the structure under investigation, or non-destructive, using some form of acoustic or electronic investigations. A summary of the advantages and disadvantages of the primary methods in use at the present time is given in the following.

Destructive methods.

Specimen Removal (concrete)

Description: in a concrete structure, this method involves extracting a specimen from the structure in accordance with ASTM C42, and determining the compressive strength and splitting tensile strength. Sawn rectangular specimens may also be extracted for determination of the modulus of rupture).

Advantages:

Working with an actual specimen from the structure in question.

Sampling requires removal of multiple specimens.

Disadvantages:

Very difficult to extract, handle, and test an intact specimen.

Destructive method, leaves a visible scar on the building.

Material strength can be altered by removal from context.

Specimen Removal (masonry)

Description: Removal of a specimen of masonry wall in accordance with ASTM C1587. Testing by ASTM C1314 (compressive strength)

Advantages:

Working with an actual specimen from the structure in question.

Sampling requires removal of multiple specimens.

Disadvantages:

Very difficult to extract, handle, and test an intact specimen.

Destructive method, leaves a visible scar on the building.

Material strength can be altered by removal from context.

Semi-destructive method.

Description: Use of a flatjack (ASTM C1196) or double flatjack (ASTM C1197) to determine *in-situ* compressive stress in a solid wall or to determine elastic modulus of

wall. In a flatjack test, a slit is sawn into the wall normal to the direction of the presumed compressive stress. The closing of the slit is measured with mechanical gages. A thin hydraulic jack is inserted into the slit and pressurized until the original configuration of the wall is restored. The hydraulic pressure is an estimate of the compressive stress in the wall.

Advantages:

Leaves only a slit in wall, which can be repaired with mortar or grout.

Gives good estimate of compressive stress or elastic modulus of wall.

Disadvantages:

Limited in scope to determinations of compressive stress and elastic modulus

Cannot be used for hollow walls or materials with voids.

Limited usefulness of information obtained from these tests.

Available non-destructive methods.

Experimental Modal Analysis

Description: In this method, an array of accelerometers is placed on a structure, or a portion of a structure, and global vibrations of the structure are excited at a number of the accelerometer locations. Based on the frequency response function (FRF) data obtained, the frequencies and modes of vibrations are reconstructed. This method requires considerable skill and specialized software to apply. Because of its global nature, it is very difficult to obtain any information about small, local defects, and even large defects do not significantly affect the global vibration response. This method works best when a baseline is obtained for identification of later deterioration, or as a tool for calibrating analytical models. A good summary of this method is given in Atamturktur (2009).

Advantages:

Provides comprehensive overview of structural behavior

Adaptable to any materials and structural configurations

Provides baseline results for later investigations

Disadvantages:

Requires skilled and educated operators

Results may be difficult to interpret, and display global behavior, rather than direct information on capacity of a structure

Method does not discriminate local defects well.

Impulse-response:

Description: This method is widely used in commercial non-destructive evaluation. In execution, it is very similar to experimental modal analysis. However, the FRF's that result from the excitation of the structure are read directly to infer material characteristics and condition. This method does not require extensive software and hardware. The interpretation of the data requires skill and experience, and the localization of defects is difficult by this method.

Advantages:

Commercially available systems

Relatively easy to implement

Provides quick output regarding response of structure.

Disadvantages:

Results may be difficult to interpret.

Very little specific information about a structure (strength, condition, defects, etc.) is obtained.

Ground Penetrating Radar.

The structure is swept along pre-established lines by a small emitter and receiver of electromagnetic waves. The waves are used to read continuously the density of the material. Specialized software is used to construct density profiles of the material along this line. This method is very useful for locating voids, especially in the ground, but can also be used for concrete or masonry walls. Choubane et al. (2003) describe the use of this method for pavement diagnosis.

Advantages:

Reveals hidden structures and features

Disadvantages

Requires skilled operator

Results may be difficult to interpret

Equipment is costly and requires specialized software.

Interference from embedded metal

Impact-Echo Method

Description: In this method a wall, slab, or beam under investigation is struck with a hardened steel ball. A receiver on the same surface detects the resulting vibrations in the slab that result from the internal echoes of the pressure waves (p-waves) in the material. The signal is converted to the frequency domain to investigate the frequencies of the internal reflections of the p-waves. For an intact, homogeneous material, the fundamental equation of impact-echo analysis is $f=\beta C_p/2t$, where C_p is the propagation velocity of the p-waves, t is the thickness of the material, f is the fundamental frequency (usually called the thickness frequency) and β is a modification factor for the shape of the specimen. Transverse echoes in a beam require modification by a $\beta < 1.0$. The size of the ball used for the impact can be calibrated to the depth of the material and to the size of the defect under investigation. Alterations to the p-wave path, resulting from layers of material, voids, defects, or inclusions, change the observed frequencies. The depth of defects can be estimated from the frequency of the return signal. This method is described in detail in Sansalone and Streett (1997) and Sansalone and Carino (1989).

Advantages:

Locates voids and defects in masonry and concrete with relative ease;

System is simple, portable, and commercially available;

Data processing depends on simple Fourier transform and filtering;

Can be applied from one side of object under investigation.

Disadvantages:

Investigation is within immediate vicinity of receiver: no global view of the condition of the structure is provided;

Requires some skill in interpreting the output;

Requires baseline measurements prior to undertaking actual measurements;

Coupling to surface is often difficult and error-prone.

Air Coupled Impact Echo Method:

Description: This method is similar to the impact-echo method. However, rather than reading the surface vibrations produced by p-waves with a displacement transducer or accelerometer, the vibrations are read using a microphone mounted one or two centimeters from the surface. Thus, the signal is air-coupled to the receiver. The microphone must be located in an enclosure that effectively seals out ambient noise and the direct sound of the steel ball striking the surface. This system does not have the coupling problems of the impact-echo method, and the receiver is very easily relocated for any following testing. This facilitates testing a large grid and other overall testing of a structure. This method is thoroughly described in Zhu (2005) and Zhu and Popovics (2007).

Advantages:

Locates voids and defects in masonry and concrete with relative ease;

System is simple and portable;

Data processing depends on simple Fourier transform and filtering;

Microphones are easy to re-position during testing;

Enhanced discrimination compared to displacement transducers.

Disadvantages:

System is local only: no global view of the condition of the structure is provided, unless a large number of data points are combined;

Requires some skill in interpreting the output;

Requires baseline measurements prior to undertaking actual measurements;

Acoustic sealing of the microphone is essential.

Spectral Analysis of Surface Waves

Description: Surface waves are excited on the structure. The advanced spectral analysis of these waves, using either single- or multi- channel acquisition methods, is used to infer the elastic characteristics of the structure or the presence of internal defects.

Advantages:

Relies on relatively simple surface measurements.

Disadvantages

Accuracy depends on distance from source;

Requires complex software and advanced analysis;

Research-level analysis method.

Sonic Pulse Velocity measurement

Description: The time required for a sonic pulse to pass through a material is measured. A grid of such measurements assists in the determination of internal defects.

Advantages:

Relies on simple surface measurements;

Measurements and software are relatively simple.

Disadvantages

Accuracy depends on distance from source;

Requires access to both sides of a slab or wall;

Information on size or depth of defects is difficult to infer.

Justification for Impact-Echo Method

Of these methods, the impact-echo method is certainly the simplest of the available methods for exploration of concrete structures. Its widespread use is both a function of its simplicity, and its capability to discriminate a significant number of defects in concrete. However, the method has shortcomings. It includes a significant amount of manual operation. It is also necessary to achieve good coupling between the transducer and the surface under investigation, either through contact pressure, gluing, or coupling media. The system is easily overwhelmed by complex data, such as larger numbers of cracks and voids in a cross-section. As a result, in its current form, it is less suitable for masonry exploration.

The use of microphones for air-coupled measurements is advantageous in that they are easy to position and locate, and they can offer an enhanced ability to defect defects compared to conventional IE displacement sensors and accelerometers, if the microphones are provided with a suitable enclosure. This method appears to be more suited to masonry exploration than the conventional procedure. This method is also significantly more amenable to automation, as the microphone, unlike an accelerometer, does not need to be coupled to the surface under investigation. As a result, the microphone is quickly and easily relocated in an automated system.

Materials and Methods

Development of equipment

The investigation of the suitability of the air-coupled impact-echo method and the experimental modal analysis method for historic structures required a substantial effort in equipment selection and in the development of equipment for enhanced testing methods. A significant effort was expended in the identification, acquisition, assembly, and testing of equipment suitable to the assessment tasks required in this project. Other effort has been directed towards programming the device operation and the signal processing. These methods and equipment are described in the following.

IEI equipment: This is a purpose-built, packaged, proprietary system for conducting impact echo analysis of concrete, with a particular emphasis on slabs. (http://www.impact-echo.com/pages/products.html). A displacement transducer is held in contact with the slab through a spring-loaded device and the slab is impacted with an appropriately-sized hardened steel spring ball. A small, conical piezoelectric element adhered to a cylinder of brass consititutes the displacement transducer. In this system, a waveform is acquired, processed and displayed using a computer-based data acquisition system. Based on information input by the user, the thickness of the material or the depth of a defect may be determined. This device was used in this project as a point of reference for comparison to the other devices that were used to obtain impact-echo measurements because of the literature supporting its use and development.

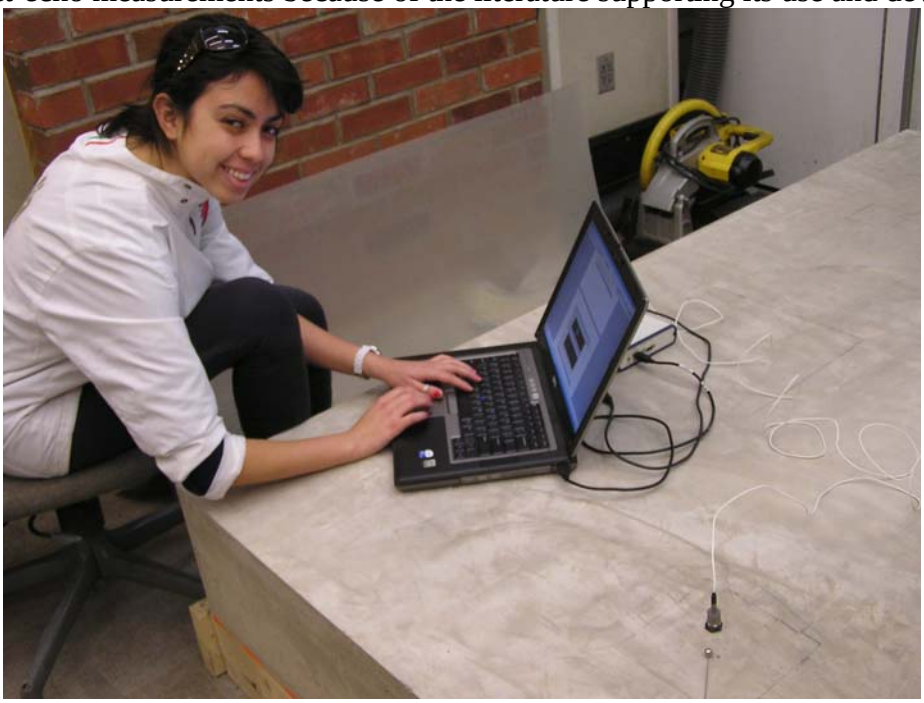

Figure 1: Accelerometer testing of a test slab, including operator, computer, data acquisition module (partially concealed behind computer and accelerometer).

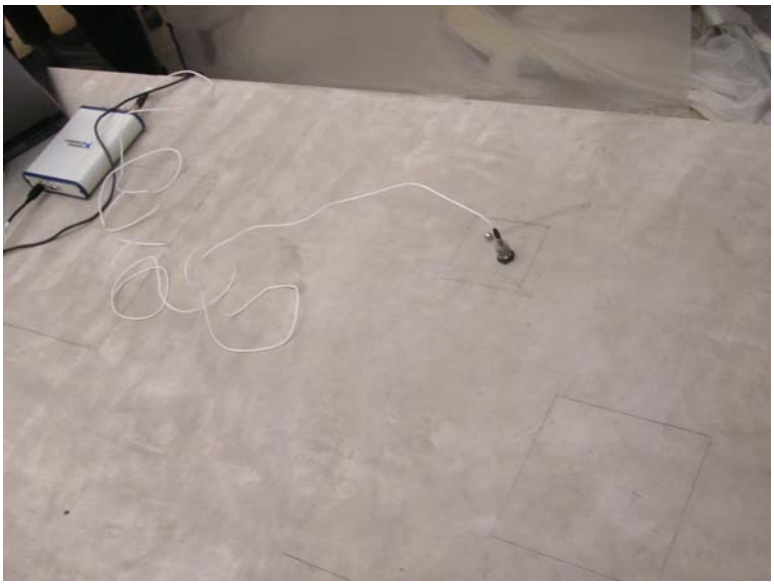

Figure 2: Accelerometer testing of slab, showing data acquisition module and accelerometer. The pencil lines on the slab represent the location of the included defects. The accelerometer is positioned over defect number 4 (described under Trial of Equipment: Laboratory).

Accelerometers: PCB model 352A78 ceramic shear accelerometers were selected for the prototype EMA/IE system. These accelerometers were chosen because their flat calibrated frequency response characteristics (± 2.5% from 5 Hz to 10 kHz, and ±5% from 10 to 15 kHz) enable their use for both EMA and IE assessments. Actual achievable frequency response is dependent on accelerometer mounting technique. Threaded stud mounts are incorporated in the accelerometers to which adhesive mounting bases are attached with a light film of silicone grease to improve vibration transmissibility. When cyanoacrylate or epoxy adhesives are used to attach the mounting pad to the material under test at each measurement point, this technique can yield acceptable performance up to 20 kHz. The application of this equipment is depicted in Figures 1 and 2.

Microphones and enclosure: PCB Y377A01 precision, ¼ in, free-field, pre-polarized condenser microphones (~ 4mV/Pa sensitivity, 4 Hz to 80 kHz at 2 dB frequency range) coupled to 1/4 in. PCB 426B03 preamplifiers (3 Hz to 126 kHz frequency range) were selected for the air-coupled system. Each microphone requires one channel of the same constant-current signal conditioning hardware required by the accelerometers to operate.

Two enclosures, depicted in Figure 3, were fabricated to support the microphones during IE assessments and to shield the microphones from ambient noise and direct acoustic waves. Enclosures are comprised of four layers. The outermost layer is a thin layer of polyurethane tape to provide exterior handling protection of the enclosure. The other three layers are based on the general enclosure details presented by Zhu and Popovics (2007). The foam and aluminum layers aid in the absorption and reflection of direct ambient noise and direct acoustic waves, and the rubber layer is intended to absorb leaky Rayleigh waves from the concrete surface and to prevent resonance within the enclosure.

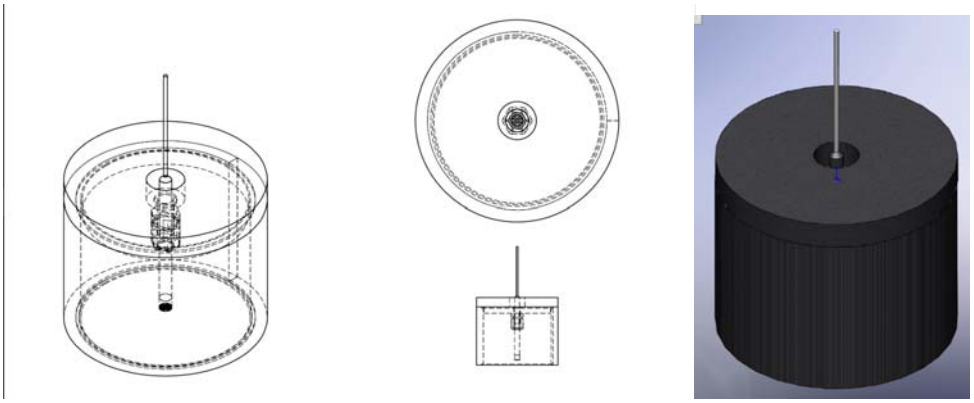

Figure 3: Custom microphone enclosure assembly.

Data acquisition and control hardware: Data acquisition and control within the prototype system is accomplished using a National Instruments (NI), model USB-4431 Dynamic Signal Analyzer with a 102 kHz bandwidth appropriate for impact echo-only, modal-only or combined impact echo/modal analysis investigations. Power to the device is supplied by the universal serial bus (USB) bus interface of a personal computer (PC) or laptop running the Windows operating system (OS). Four channels of simultaneously acquired analog input, one channel of analog output and eight digital input/output (I/O) lines can be flexibly configured to offer a number of testing configurations with this setup. Analog input lines are alternating current (AC)-coupled to provide the excitation and signal conditioning for integrated electronics piezoelectric (IEPE) accelerometers, microphones and other piezo-based devices. NI compactDAQ 9401 (twenty four channel digital I/O) and 9481 (four channel AC/DC relay modules) housed in USB bus powered carrier housings expand on the capabilities of the 4431 module to provide full automation of the impactor equipment described. Figure 4 shows schematically the use of the dynamic signal analyzer.

Data Acquisition and Control Software: A large portion of the combined EMA/ACIE prototype system development work has been done with the NI Signal Express 2009 interface, which allows flexible setup of sensor/hardware configurations to quickly obtain time and frequency domain signals to guide software development efforts using the NI LabVIEW 2009 Professional Development System with the Sound and Vibration Toolkit, and Diadem supporting software. As the project progressed, discussions with ABSignal, the developers of ModalVIEW software for automation of EMA with NI dynamic signal analyzer hardware, led to the realization that a plug-in module for combined EMA/ACIE work with the prototype system hardware is possible, and further development proceeded along these lines.

Modal Analysis Software: The modal analysis software used is the Beta version of ModalVIEW. This is a package of software routines developed with the LabVIEW compiler for use with National Instruments data acquisition software. It was chosen for its compatibility with other general-purpose data acquisition hardware and software, because this characteristic facilitates the development of simultaneous processing capability for modal analysis and for other dynamic processes, such as impact-echo, and air-coupled impact echo. Given a sufficient number of points, the program can calculate the natural frequencies of the structure and the most probable mode shapes of the natural frequencies, on the basis of the calculated frequency response functions.

Figure 4: Prototype EMA/IE system.

Automated Impactor: A prototype automated impactor system was developed to explore the possibilities for automating the impact delivery. The system is comprised of a single and multiple impactor platforms. Both platforms allow the use of barrels that have been developed for hardened steel ball impactors ranging in diameter from 1/8 in. to 2 in. and a common automation setup. As many as six barrels can be used with the multiple barrel impactor, and a barrel is isolated for use by opening and closing ball valves emanating from a manifold. Barrels are interchanged quickly by hand using aluminum pipe unions and custom-built hardware for housing the barrel. Figure 5 details important aspects of the single impactor setup. Balls are loaded into the barrel manually and then a metal sleeve is slid over the ball chamber machined into the barrel. A permanent pin backstop in the chamber keeps the ball from moving backwards, and a movable pin connected to a tubular solenoid keeps the ball from moving forward until the solenoid is actuated. Prior to firing the ball, pressure level to an accumulator tank is set by software using an electronic proportional regulator connected to a portable air compressor unit. An impact event occurs upon depression of the momentary switch integrated into the handle of the single impactor device and the manifold of the multiple impactor devices.

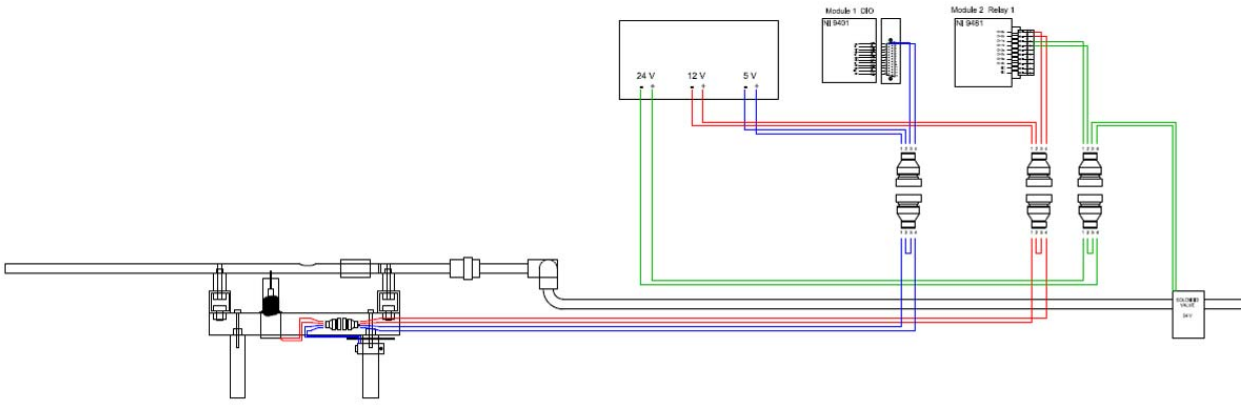

(a)

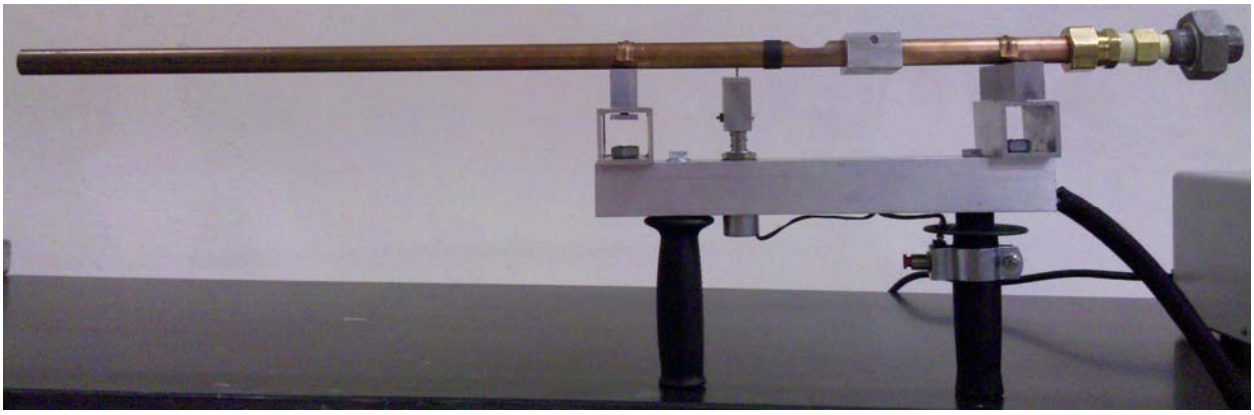

(b)

Figure 5: Automated impactor: (a.) view of initial prototype and (b.) schematic diagram.

A further development of the prototype to implement automated impact-echo scans of floors is shown in Figure 6. The configuration in the figure is similar to the implementation of the system in a laboratory or field environment, including the microphone enclosure and microphone. Prior to firing a steel ball impactor, pressure level to the accumulator tank is set by software using an electronic proportional regulator connected to the portable air compressor unit. An impact event occurs upon depression of the momentary switch integrated into the handle of the single impactor device shown here and the manifold of the multiple impactor devices. The momentary switch triggers the software interface with a digital high signal which in turn: energizes the tubular solenoid via electromechanical relay to retract the forward chamber pin, opens a solenoid valve via electromechanical relay to supply a burst of compressed air at the desired pressure and for the desired length of time needed to achieve the desired dynamic characteristics of the impact event, and readies the dynamic signal acquisition hardware for triggering via an infrared diode emitter/receiver sensor circuit at the exit of the barrel (not shown in the figure). The high speed camera is used for the measurement of the exit velocity and for the determination of the waveform of the impact.

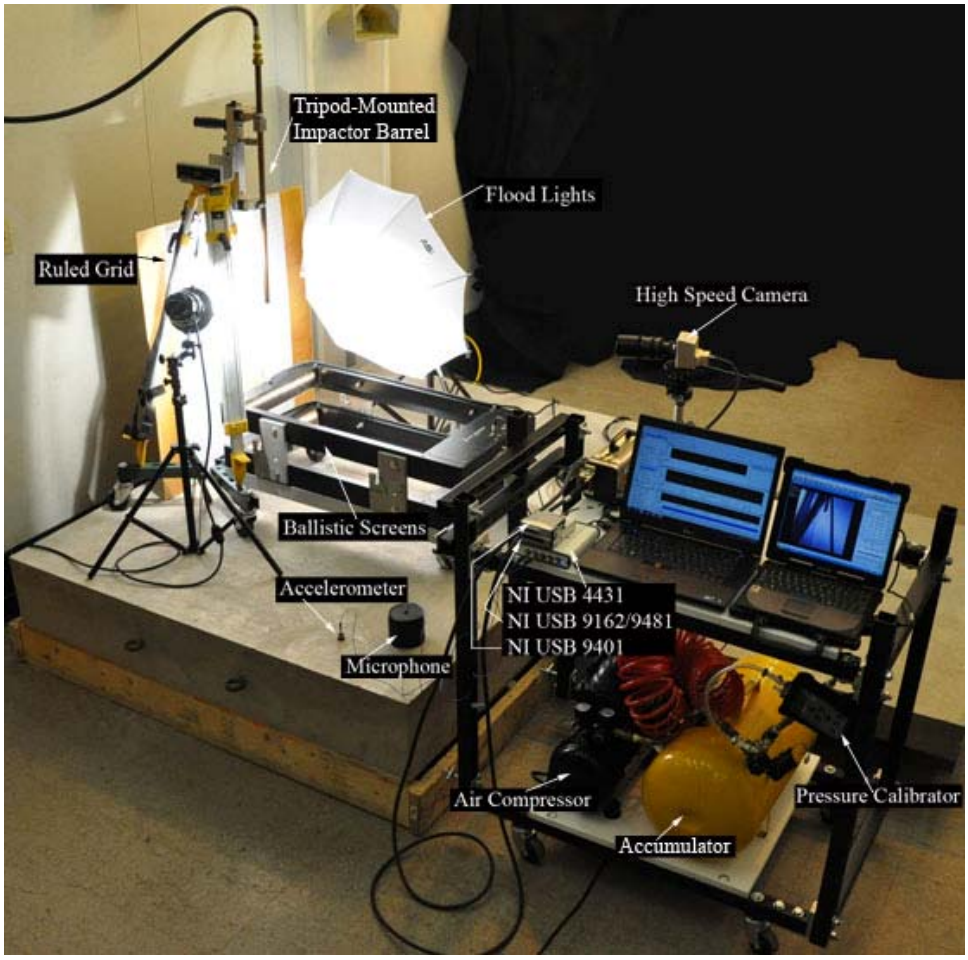

Figure 6: Automated steel ball impactor prototype and impactor calibration equipment arrangement. Interconnection cables not shown for clarity.

Trial of equipment: laboratory

Beam Specimens

Beams of dimensions 6" (width) × 9" (depth) × 76" (length) were built. The beams were lightly reinforced with 2 #3 reinforcing bars. The three beams included a control, without intentional defects, a beam with three small rock pockets, meant to simulate areas of poor consolidation, and a beam with three foam inserts, simulating voids. The beams were subjected to modal testing to determine the frequencies and mode shapes of vibration. The beams were also subjected to impact echo testing, using IEI Equipment, using accelerometers, and using microphones as described above. The target concrete strength of the beams was 4500 psi.

Initial trial slab 48" × 48" × 5"

An initial trial slab was built in the laboratories at Penn State University. This slab had dimensions of 48" × 48" and a thickness of 5". The target concrete strength for the slab was 4500 psi. The concrete was delivered by a local ready-mix supplier and compacted using hand-held mechanical vibrators. The slab had no intentional defects. The slab was tested with a 3/32" vinyl composition tile adhered to the top surface, and without the tile, to assess the effect on the signal of testing through tile.

Larger Slab with Embedded Defects

The larger trial slab was built with dimensions of 59" × 78 1/2" × 10". Following the scheme in Zhu and Popovics (2002), the slab had eight concealed defects. A sketch of the distribution of the defects is shown in Figure 7 and 8. Construction of the slab was similar to that of the slab described directly above.

Impact-echo Testing of Beams and Slabs

An initial series of tests was conducted by the impact-echo method, using the pre-packaged IEI equipment described above. This testing program included testing of the beams and the large slab with defects. The impact echo testing of the beams and the large slab was repeated using accelerometers and the USB-4431 interface. The testing of the large slab was also repeated using the microphone sensors.

Beam Tests (IEI Equipment): Beam tests were conducted using two forms of impact-echo. Because the signal is disturbed by the additional internal reflections off the side walls of the beam cross section, it is not possible to speak of a thickness frequency for transverse tests on a beam. Instead, a Mode I, Mode II and a Mode III frequency are calculated. For an impact at the top of the beam, mode 1 is direct reflection off the bottom of the beam; Mode II and Mode III include reflections from the sidewalls of the beam.

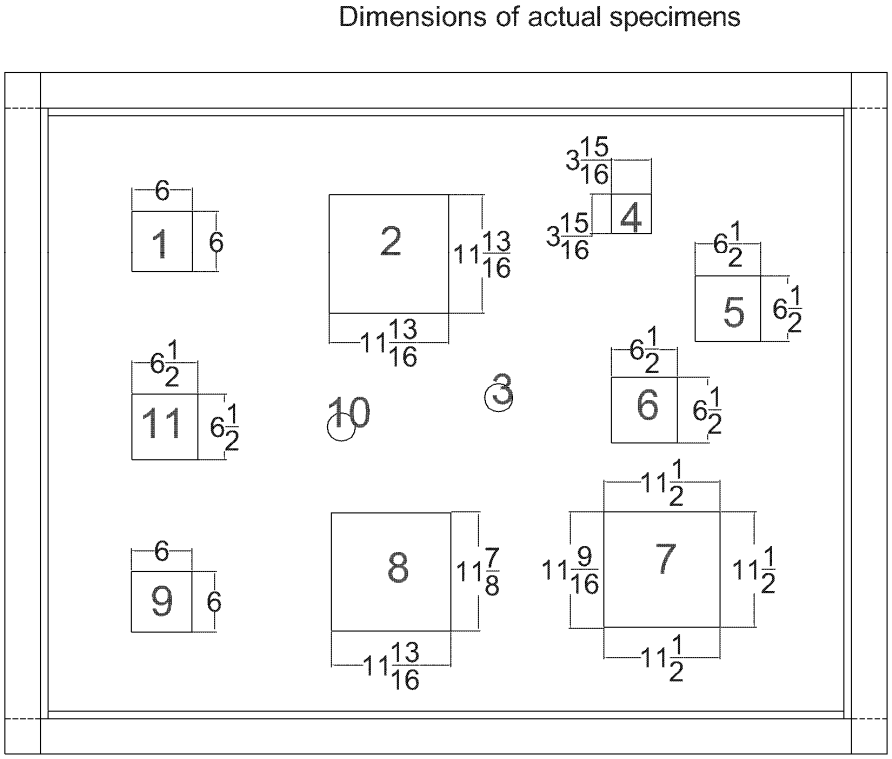

Figure 7: Horizontal dimensions of embedded slab defects (dimensions in inches).

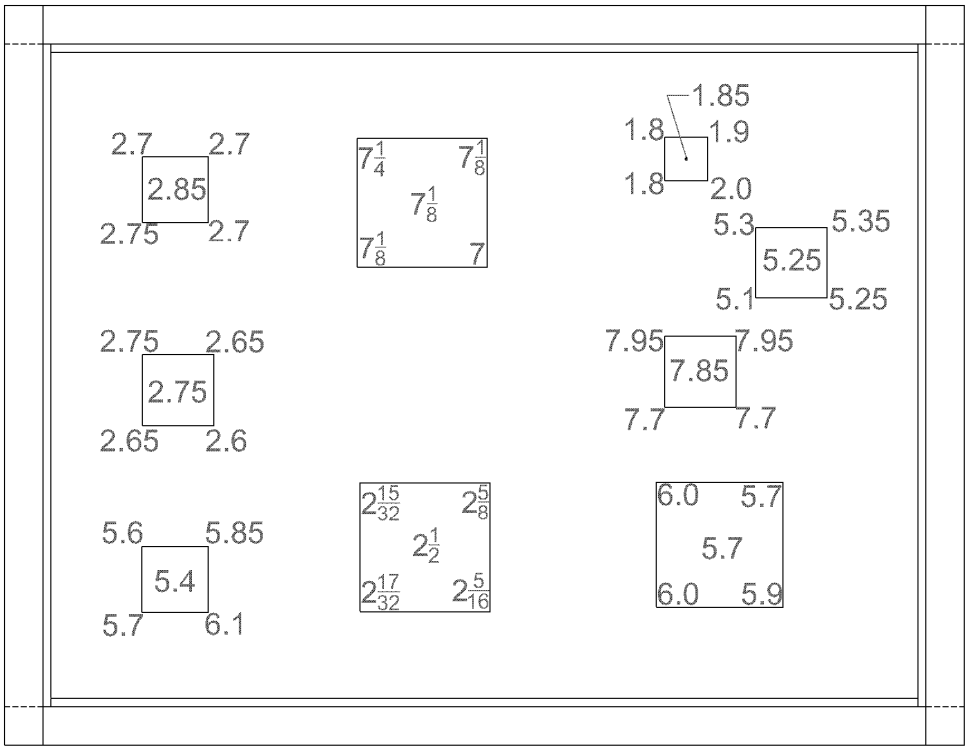

Figure 8: Depth of embedded slab defects (inches).

The velocity of the p-wave was determined to be 3500m/sec based on a direct measurement done with two displacement transducers clamped at 30 cm apart. This velocity applies to all the three beams. The calculated p-wave velocity, using the concrete strength and density and a Poisson's ratio of 0.10, is 3400 m/s. For beams, the p-wave velocity is modified by 0.95 to account for internal reflections off the walls of the beam. Three points were tested on the defect-free beam. One point was located at midspan, and the other two were located 19" from each end. Five points were tested on the beam with rock pockets: three correspond to the defects and two points have been chosen on location that has no defects, except the presence of the re-bars. The defects were located at 10", 38", and 65" along the beam. Additional points not over defects were tested at 24" and 52." The Mode I frequency was expected to be 7.4 kHz. The dimensions of the rock pockets vary. At 10" and 65", they were located approximately at 6.5cm from the bottom of the beam, and the expected frequency due to their presence is expected at 10.4 kHz.

Five similar locations were tested on the beam with foam inclusions. Three correspond to the defects and two points have been chosen on location that has no defects, except for the presence of the reinforcing bars. The defects are located at 10", 38", 65" and the points without defects were located at 24" and 52" from the left side of the beam. The fundamental frequency was expected at 7.4 kHz. . For the foam inclusions located at 4.5 cm from the bottom of the beam, the expected frequency was 9.2 kHz.

Slab (IEI Equipment): The smaller slab was subjected to impact-echo testing using three different devices. The first was the pre-packaged displacement transducer and data acquisition card combination, manufactured by IEI. This equipment was positioned near the center of the slab. The slab was also tested using the accelerometer connected to the NI data acquisition card. Parameters used for this test included a sampling rate of 25000 kHz, 1024 samples total, giving a window of 41 ms. The slab was later tested using the microphone and microphone enclosures.

Slab with Defects (IEI Equipment): The experimental slab was cast from concrete with a nominal compressive strength of 4500 psi (31 MPa), and a density of 145 lbs/ft^3 (2300 kg/m^3). As such, the modulus of elasticity is expected to be approximately 26.3 GPa, resulting in a calculated p-wave velocity of 3380 m/s. A testing grid was superimposed on this slab to locate the equipment used in testing. The spacing of the grid was 6" × 6". The slab was tested with conventional IEI equipment, with accelerometers mounted to the surface of the slab with microcrystalline wax, and with a microphone transducer.

Beams (accelerometers): The tests were intended to assess the Mode I frequency found in an impact echo test of the beam without any .defects. Following this, the beams with defects were tested, both in the location of the suspected defect and in a location where defects are not present. The characteristics of the beams and the testing program are similar to the program conducted using the IEI equipment.

Slabs (accelerometers): The large slab with defects was tested by the impact-echo method, using accelerometers to detect vibrations. The acquisition rate was set to 51 kHz, with an anti-aliasing filter installed. 2000 data points were collected, including 500 pre-trigger points. The results were transformed into the frequency domain, to plot a spectrum, for evaluation of the frequency

of the return signal. The characteristics of the slab and the testing program were similar to that of the program using IEI equipment, described above.

Slabs (microphones): The large slab with defects was tested by the impact-echo method, using accelerometers to detect vibrations. The characteristics of the slab and the testing program were similar to that of the program using IEI equipment, described above. The characteristics of the data acquisition were similar to the accelerometer testing described directly above.

Modal Testing of Beams

The beam specimens were further tested by modal analysis, using the same equipment as was used for the impact-echo testing by accelerometer. In the testing, five locations were chosen for the accelerometers, by subdividing the span of the beam into seven equal length segments. In the testing, the beam was impacted at point 2, the point closest to one of the supports, and the accelerometers were moved from test to test. After the beam had been tested at each of the seven points, a complete picture of the frequencies and mode shapes of the vibration of the beam can be determined and reported. A beta version of the software ModalVIEW, which is compatible with the other National Instruments LabVIEW-based software used in this project, was used for the purpose of reconstructing the mode shapes of the vibration of the beams.

Trial of Equipment (Field)

The procedures described above were implemented in a number of different tests conducted on components of historic buildings at Wright-Patterson AFB, OH. The buildings, currently designated Building 18F and Building 19, are both contributing resources in the Wright-Patterson AFB Area B Historic District. The two buildings, described below, have been documented by the Historic American Engineering Record (HAER). Their HAER numbers are given below.

> Building 18F (Power Plant Cold Rooms). Originally built in 1945 to house aviation research functions in aircraft power plant testing under cold conditions, Building 18F has a central high bay and lateral mezzanines formed in reinforced concrete. Later additions include additional mezzanines in light steel framing. (HAER OHIO,29-DAYT.V,1AN-2).
>
> Building 19 (5 Foot Wind Tunnel Building). Built in 1927 with corrugated metal siding, and completed in its present form, with brick infill walls, two years later, Building 19 has housed the 5 foot wind tunnel since 1929. The tunnel was used to conduct experiments on prototypes of early aircraft through the period immediately following World War II. The building is constructed of steel framing on concrete pedestals supporting a trussed roof. The walls consist of infill 2-wythe brick walls and large steel sash windows. (HAER OH-79-B) An exterior view of this building is shown in Figure 9.

Figure 9: Building 19, Area B, Wright-Patterson AFB.

Tests at Building 18F concentrated on one bay of a structural reinforced concrete floor slab, supported by reinforced concrete joists. The testing was conducted in Room 223, as the walls of the room include an entire bay, approximately 16'-6" × 18'-6". The tests included a variety of measurements along a grid of points in the single bay of the floor system. The measurements included impact-echo, using the IEI equipment, air coupled impact-echo, modal testing, and a semi-automated procedure combining the features of impact echo analysis with those of modal analysis. These procedures will be briefly described below.

A grid of points was laid out with 9 grid lines in the east-west direction, spaced at 2 foot intervals, and 5 grid lines in the north-south direction, corresponding to midspan of the slab between joists and the centerline of the joists. As the spacing of the joists was irregular, this resulted in the grid spacing being slightly irregular. Each point in the grid was tested by the impact-echo method, using a ball of approximately 10 mm diameter. Data was collected at each point using the IEI equipment and using microphones and the air-coupled impact echo method. In the microphone testing, the microphone was set to 15 cm from the surface of the slab. The sensitivity of the microphone used, 4.51 mV per Pa, was entered into the data acquisition program. Three frequency domain records were obtained at each tested point, and stored for later processing. A couple of accelerometer tests were conducted at the same location as the microphone tests to corroborate the results of the microphone testing. This series of tests was conducted on March 16, 2010. The grid is shown in Figure 10.

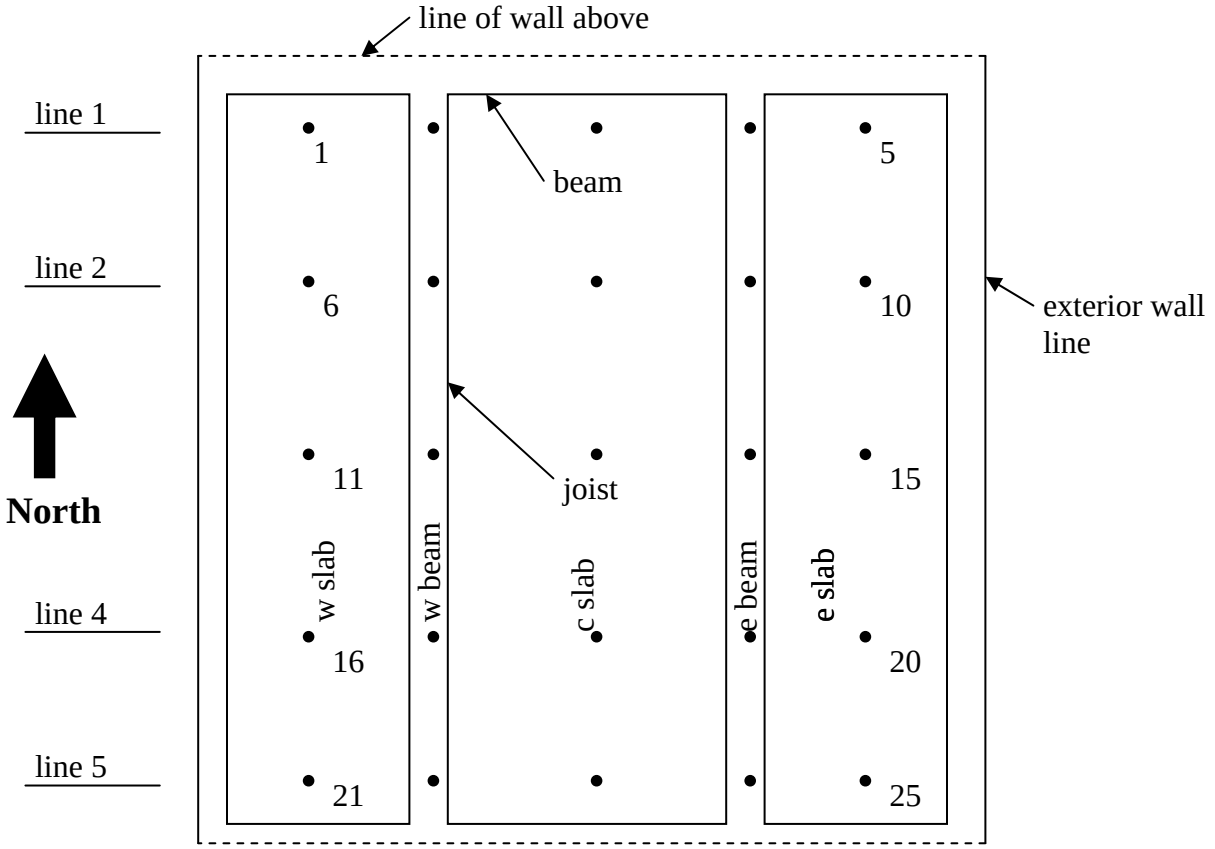

Figure 10: Grid points on floor slab: Building 18F.

Grid points are referenced either as a combination of location and line, such as W-beam 4, for a point lying along the west beam at grid line 4, or by a specific number (required for modal analysis input), such as point 11.

A modal test was conducted on two sets of points in the previously defined grid. Using alternate points in the north-south grid results in 25 grid points, which is sufficient to obtain good modal results for a system on the scale of this floor system. Grid points were numbered as shown in Figure 10.

Testing was accomplished using fixed accelerometer locations, and by roving the hammer. Accelerometers were permanently located at points 11 and 13, which include the center of the slab. Each successive point was struck by the hammer to generate a trigger event, and the vibration at the two accelerometers was recorded. Following this, the hammer was moved to the next position, and the slab was struck again. Three records were obtained at each test point, and checked for coherence. This test was completed on the morning of March 17, 2010.

An additional test involved the development of the ball firing system. The system was pressurized and used to generate the impacts for a further round of impact-echo testing. Again, all of the response data was saved for later viewing and interpretation. Throughout this test, the two accelerometers remained at points 11 and 13. This testing was completed on the afternoon of March 17, 2010

Additional tests were performed on one of the central columns in Building 18F. Air-coupled impact echo tests were completed at four different levels of the column. In the accelerometer based procedure, an accelerometer was adhered to each side of the column, using a micro-crystalline wax. The column was impacted near the accelerometer, and the acceleration results were transformed to the frequency domain for interpretation. The air-coupled procedure was similar, but a microphone enclosure with a microphone was substituted for the accelerometer. This testing, completed on March 18, 2010, is illustrated in Figure 11.

Figure 11: Air-coupled impact-echo test on a column: Building 18F.

Many of the plain concrete pedestals supporting the columns in Building 19 display patterns of cracking. The most commonly occurring crack is a horizontal crack through the pedestal at approximately mid-height, but in other cases diagonal cracking initiating at the horizontal crack and stand-alone diagonal cracking are observable. Impact-echo testing was performed on a number of the pedestals, some with observable cracking, and some without observable cracking. A sample of the pedestals in Building 19, was also tested using air-coupled impact-echo analysis. The pedestals have dimensions of 12" × 24" in plan, and a height of 72" above the floor. The pedestals were tested at three elevations across the 12" width, along the 24" length, and also tested once along the height. The aspect ratio of the pedestal in the 12" (transverse) direction qualifies it to be considered as a plate structure, and is the most favorable for impact-echo testing, while in the perpendicular direction, the pier is considered as transitional between a plate and a rod. In testing along the height, the pier is considered to behave as a rod. The pedestals have designations N (north) or S (south), and are numbered from 1 to 10 beginning at the east end of the building. The pedestals on the north side of the building display the greatest damage, while those on the south side appear substantially undamaged. The pedestals tested were 3N, 6N, 7N, 8N, and 8S. Figure 12 illustrates the testing procedure.

Figure 12: Air-coupled impact-echo testing of pedestal in Building 19.

The two wythe brick infill walls of Building 19 were subjected to further air-coupled impact-echo testing. The walls are built in common bond, with six courses of stretchers, or bricks laid with the long face outwards, followed by a single header course, that is a row of through bricks, with the short face showing to the outside. This construction is shown in the photograph in Figure 13. The purpose of this testing was to determine the suitability of this method for the assessment of masonry structures. In general, masonry structures, having internal discontinuities, are more difficult to assess using this method, due to further difficulties in interpreting the spectra that result from the tests. The exterior wall of the building was subjected to a number of tests on a predetermined grid. Two bays of infill wall were tested, each according

to the grid shown in Figure 14. The maximum height that could be reached using a stepladder was nine feet, so no tests were conducted above that level.

Figure 13: View of one infill panel of the North wall of Building 19.

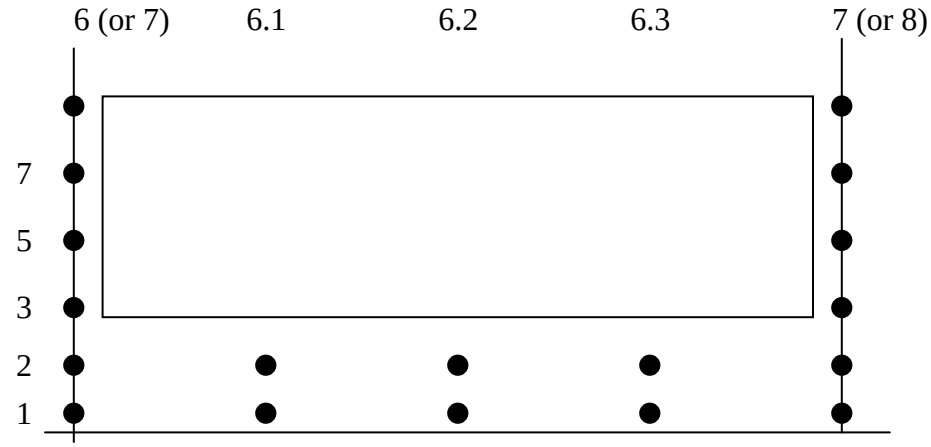

Figure 14: Layout of testing grid on exterior wall of Building 19.

Two infill panels were tested in Building 19. These panels were located on the north wall between piers 6 and 7 and piers 7 and 8. The schematic diagram above shows the locations that were tested in each panel. Each location is designated by its height, 1, 2, 3, 5, 7, or 9 feet above grade, and by its horizontal location between piers 6-8, as shown on the schematic. There was widespread damage to these walls, with most of the damage located in the piers between the windows, where the weight of the wall above the windows is transmitted to a small area of masonry.

Results and Discussion

Conventional Impact-Echo Results

Beams

The beams were tested using the IEI system in accordance with the procedure described under Materials and Methods. The Mode I frequency was found to be 7.3 kHz. Corrected for the 1.5 (dimension in the direction of sound propagation/perpendicular dimension) aspect ratio of the beam cross-section, this frequency results in a wave velocity estimate of 4200 m/s (see discussion of impact-echo method in the Background section). This was the fundamental frequency apparent in all tests, including defect locations and defect-free locations. As shown in Figure 15, a second peak was apparent in specimens with rock pockets, indicating a disturbance to the wave path at 10 kHz, representing approximately 3/4 of the depth.

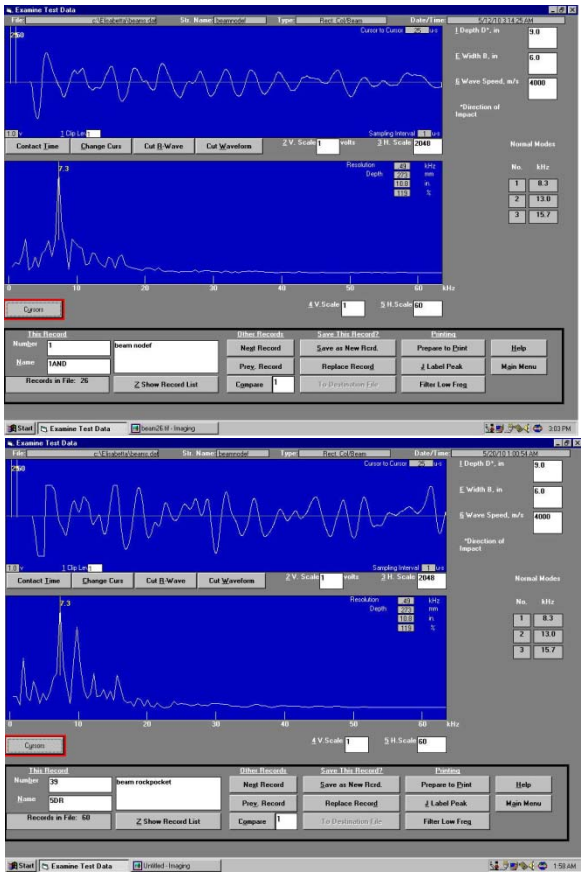

Figure 15: Impact-echo results for defect-free slab (above), and slab with a simulated rock pocket (below).

Slab with Included Defects

Table 1 shows a comparison of the expected and observed Mode I frequencies in the tests of the slab with defects. In the general description line, the defect size is generally indicated as >t (slab thickness), <t, or ≈t indicates the relationship between the horizontal dimension of the defect and the slab thickness t. It is observable from Table 1 that the range of the observed fundamental frequencies was reasonably close to the expected fundamental frequency for larger and deeper defects, and for the no defect condition. This can be seen especially at points 2, 3, 6, and 10. However any size of defect close to the surface of the concrete created unexpected results. Normally, a very high frequency should be observable as a result of this condition, while in most cases, smaller and shallower defects tended to shift the fundamental frequency to a lower value, which is generally not an expected result in impact-echo analysis.

Table 1: Conventional impact-echo results of slab with defects

Point	1	2	3	4	5	6	7	8	9	10	11
general description	<t	>t	no defect	<t	<t	<t	≈t	≈t	<t	no defect	<t
depth (in)	2.8	7.1		1.8	5.2	7.8	5.7	2.1	5.4		2.8
funda-mental frequency (kHz)	5.9	9.3	8.3	8.3	5.4	11.2	5.4	3.4	5.4	8.3	4.9
Expected funda-mental frequency (kHz)	23.1	9.1	6.1	35.6	12.7	8.4	11.6	12.5	22.4	6.7	23.9

Two explanations for this phenomenon are possible. The first is that the dominant mode of response is flexural vibrations of the delaminated area above the defect, and that the displacement transducers are detecting this vibration mode instead of the p-waves reflecting from the surface of the imperfection. A further possibility is that these observations represent the existence of a diffracted path for p-waves around the defect, and not the reflected p-waves from the surface of the disturbance.

The screen shot in Figure 16 represents the response of point 9. In addition to the fundamental frequency, there is a large peak at about 15 kHz, and another peak at the expected value of 22 kHz. Because the system only picks the largest peak to identify as the fundamental frequency, it suggests that some further modification of the data or the intervention of a skilled operator is necessary to use this system effectively.

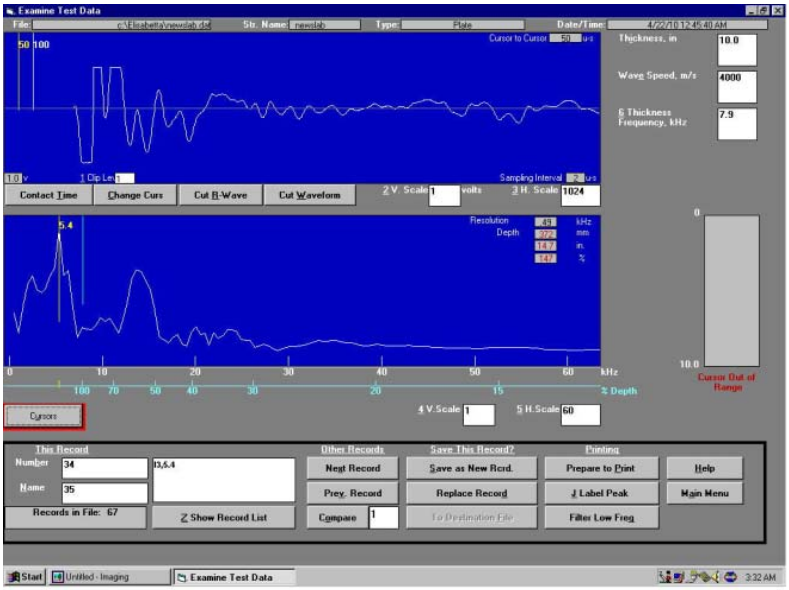

Figure 16: Example slab results for IEI impact-echo equipment.

Accelerometer Results

Beams

Table 2 shows the results of the beam tests using accelerometers in conjunction with the data acquisition system developed for this project (See Data Acquisition and Control in the Materials and Methods section). Three points were tested on the defect-free beam in order to prove the repeatability of the results. One point is located at midspan, and the other two are located 19" from each end. The expected Mode I frequency is 7.4 kHz and the frequency obtained from the test is 7.8 kHz. Taking into consideration the reinforcing bars, this is acceptable agreement because the presence of the reinforcement shifts the frequency a little bit higher. There are two additional significant peaks, one at 9.7 kHz and the other one at 12 kHz. They are mostly likely the result of the presence of the rebars.

Five points were tested on the beam with simulated rock pockets: three correspond to the defects and two points have been chosen on location that has no defects, except for the presence of the rebars. The defects are located at 10”, 38”, 65” and the points not over defects are located at 24” and 52” from the left side of the beam. The fundamental frequency is expected to be 7.4 kHz and the tests show the first peak at 7.8 kHz. The dimensions of the rock pockets vary. At 10” and 65”, they are located approximately at 6.5cm from the bottom of the beam, and the expected frequency due to their presence is 10.4 kHz. The experiments demonstrate a second peak, due to the rock pocket, at 11 kHz. At 38” from the left side, the rock pocket is located approximately at 5.5 cm from the bottom of the beam and the expected is 9.8 kHz. The results show a second significant frequency is at 9.8 kHz. The nature of the rock pockets makes them relatively easily detectable, in the sense that they are compact and even though there is a small shift in frequency, the p-wave is almost be reflected from them. There is a third significant peak at 12 kHz, which matches that detected in the beam with no defect. This is most likely due to a cross sectional mode of the beam. Finally, for the points that have no defects, a second mode appears at 9.8 kHz

and 10 kHz. This is most likely due to reflection from the faces of the beams, as in the case of the beam with no defect.

Table 2: Accelerometer results for beams

	POINT	EXPECTED FUNDAMENTAL FREQUENCY (kHz)	DEPTH OF DEFECT (cm)	EXPECTED DEFECT FREQUENCY	1^{ST} MODE	2^{ND} MODE	3^{RD} MODE
beam1,no def,19"	1	7.4	none	none	7.8	9.7	12.0
beam1,no def,38"	2	7.4	none	none	7.8	9.7	12.0
beam1,no def,65"	3	7.4	none	none	7.8	9.7	12.0
beam rock, def @10"	1	7.4	0.17	9.8	7.8	11.0	12.2
beam rock, def @38"	2	7.4	0.17	9.8	7.8	9.8	12.0
beam rock, def @65"	3	7.4	0.17	9.8	7.8	11.0	12.0
beam rock, no def, 24"	4	7.4	none	none	7.8	10.0	12.2
beam rock, no def, 52"	5	7.4	none	none	7.8	9.8	12.0
beam foam, def @10"	1	7.4	0.18	9.2	6.0	9.8	12.0
beam foam, def @38"	2	7.4	0.18	9.2	7.8	9.5	12.0
beam foam, def @65"	3	7.4	0.18	9.2	7.8	9.3	11.5
beam foam, no def, 24"	4	7.4	none	none	7.8	9.5	12
beam foam, no def, 52"	5	7.4	none	none	7.8	9.5	12

Five similar locations were tested on the beam with foam inclusions. Three correspond to the defects and two points have been chosen on location that has no defects, except the presence of the reinforcing bars. The defects are located at 10”, 38”, 65” and the points on no defects are located at 24” and 52” from the left side of the beam. The fundamental frequency is expected at 7.4 kHz and the tests show the first peak at 7.8 kHz, except for the point at 10” where the fundamental frequency has been measured at 6 kHz. For the foam inclusions located at 4.5 cm from the bottom of the beam, the expected frequency is 9.2 kHz. The experiments demonstrate a second peak at approximately 9.5 kHz for all defect locations. There is a third significant peak at 12 kHz that matches the one detected in the beam with no defect and the one detected in the beam with rock pockets. This is most likely due to a cross sectional mode of the beam. Finally, for the points that have no defects, a second mode appears at 9.8 kHz and 10 kHz. This is most likely due to reflection from the faces of the beams, as it was for the previous cases.

The general finding of the beam tests is that there is acceptable agreement between the expected results and the actual results. The tests were able to determine the depth of the rock pockets and the foam inserts in the beams with reasonable precision. Reflection modes in a beam and modes that are produced by reflections from the reinforcing steel have to be discriminated from the modes produced by the defects in further testing.

Slab with Included Defects

Table 3: Accelerometer testing for slab with defects

POINT	EXPECTED FUNDAMENTAL FREQUENCY (kHz)	DEPTH OFDEFECT (cm)	EXPECTED DEFECT FREQUENCY	1^{ST} MODE	2^{ND} MODE	3^{RD} MODE
1	6.7	7.23	23.2	5.9	14.0	24.0
2	6.7	18.40	9.1	none	13.0	17.5
3	6.7	25.00	6.7	8.0	10.0	12.5
4	6.7	4.70	35.6	7.2	15.0	22.0
5	6.7	13.20	12.7	5.1	13.2	20.0
6	6.7	19.90	8.4	none	11.2	12.2
7	6.7	14.40	11.6	none	14.2	16.2
8	6.7	6.32	26.5	3.6	10.0	12.4
9	6.7	13.70	12.2	11.0	12.5	14.5
10	6.7	25.00	6.7	8.0	12.5	15.5
11	6.7	7.00	23.9	5.0	10.8	12.0

The results from the accelerometer-based impact echo testing of the reinforced concrete slab with embedded defects are summarized in Table 3 above. The defects varied in size and depth and the ability of the system to capture these defects unambiguously also varied. Several general observations are possible concerning this series of tests. The first is that the defect-free portions of the results returned a clear first mode at the expected fundamental frequency of the slab, although the first mode was not the mode which returned the greatest amplitude in most cases. The greatest amplitude was almost always in the 12 kHz-16 kHz range, and is most probably associated with patterns of reflection from the reinforcing steel. For small defects close to the surface, such as at points 1, 4, 8, and 11, a shift towards a lower first mode frequency is apparent. This is thought to be due to diffraction around the defect, which lengthens the path of the pressure wave. The higher modes at these locations did not consistently show the presence or depth of the defect. Larger and deeper defects were discriminated better by this test. The frequency associated with the total slab thickness tended to vanish at these locations, and a higher frequency first mode was observed. Examples are Points 2, 6, and 7, for which the results can be seen in Table 3.

Microphone (air-coupled) Testing of Slab

Table 4: Results of microphone testing of slab with defects

POINT	EXPECTED FUNDAMENTAL FREQUENCY (kHz)	DEPTH OFDEFECT (cm)	EXPECTED DEFECT FREQUENCY	1^{ST} MODE	2^{ND} MODE	3^{RD} MODE
1	6.7	7.23	23.2	5.2	9.8	24.0
2	6.7	18.40	9.1	9.8	10.8	14.2
3	6.7	25.00	6.7	8.0	10.7	12.1
4	6.7	4.70	35.6	17.1	19.5	22.0
5	6.7	13.20	12.7	15.5	16.1	17.2
6	6.7	19.90	8.4	9.8	13.0	14.2
7	6.7	14.40	11.6	14.4	15.5	16.2
8	6.7	6.32	26.5	9.8	10.7	12.1
9	6.7	13.70	12.2	14.2	16.1	17.1
10	6.7	25.00	6.7	8.0	12.5	15.5
11	6.7	7.00	23.9	5.4	10.8	12.2

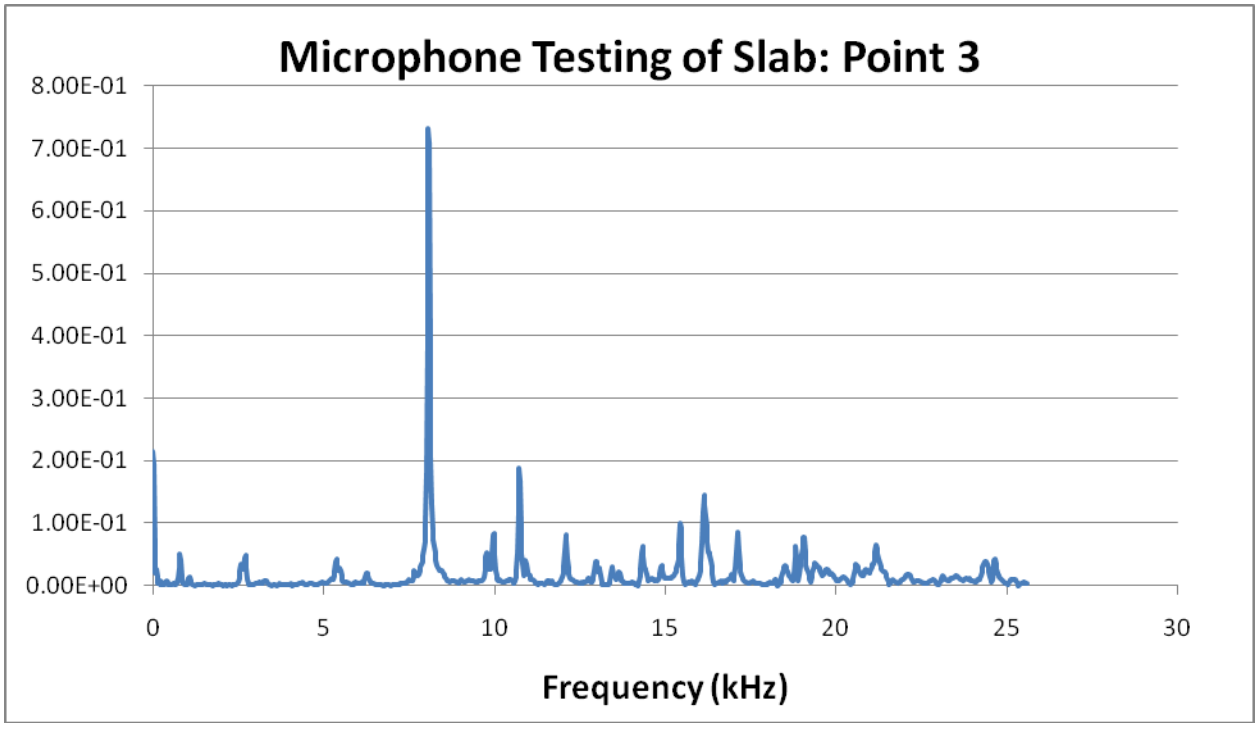

Figure 17: Air-coupled impact echo results from point 3 (defect-free)

The results of the air-coupled impact echo testing of the slab are shown in Table 4. The observed fundamental frequency in all cases was 8.0 kHz. Due to this observation, the actual defect frequencies are expected to be similarly 15-20% greater than the expected values. The

fundamental frequency was more or less dominant, depending on the presence of defects. In general, the values shown in the table of microphone results are comparable to the accelerometer results, although the microphones present good results for a few more of the defects. In the absence of defects, such as at Point 3, the fundamental frequency was clearly dominant (Figure 17). In general, the identification of shallow defects based on frequency alone was difficult, while the deeper defects followed the expected defect frequencies with reasonable accuracy. A plot of the results for defect 7 shows the expected behavior (Figure 18). The attenuation of the thickness frequency (8.0 kHz) is clear evidence of the presence of a defect, while the large amplitude peaks clustered around 14 kHz are very close to the expected defect frequency.

On the other hand, the results for Point 1 (Figure 19), while the frequency data are very difficult to interpret, clearly show evidence of disruption of the signal. The high frequencies associated with shallow defects generally have lower amplitudes and are difficult to compare to the thickness frequency or the defect frequencies of deeper defects.

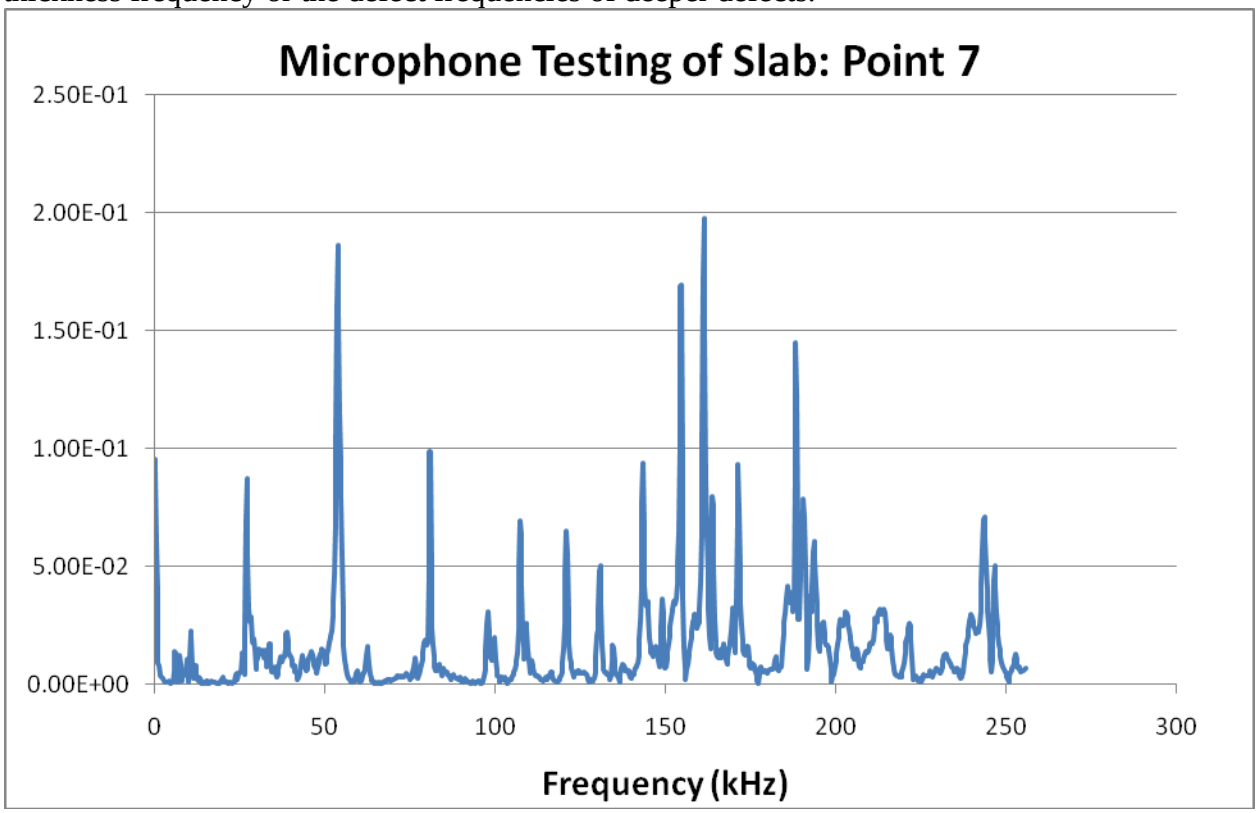

Figure 18: Impact-echo results for point 7 (defect at mid-depth of slab).

The results for point 1 show some attenuation of the thickness frequency and a pattern of many additional higher frequency peaks. Although there is a definite peak around the expected defect frequency of 23 kHz, it is not possible in looking at this plot without prior knowledge of the depth of the defect to identify this peak as corresponding to the defect. At this point, it is only possible to infer the presence of a defect. Some further work with the patterns produced by various defects may make more discrimination of defects possible.

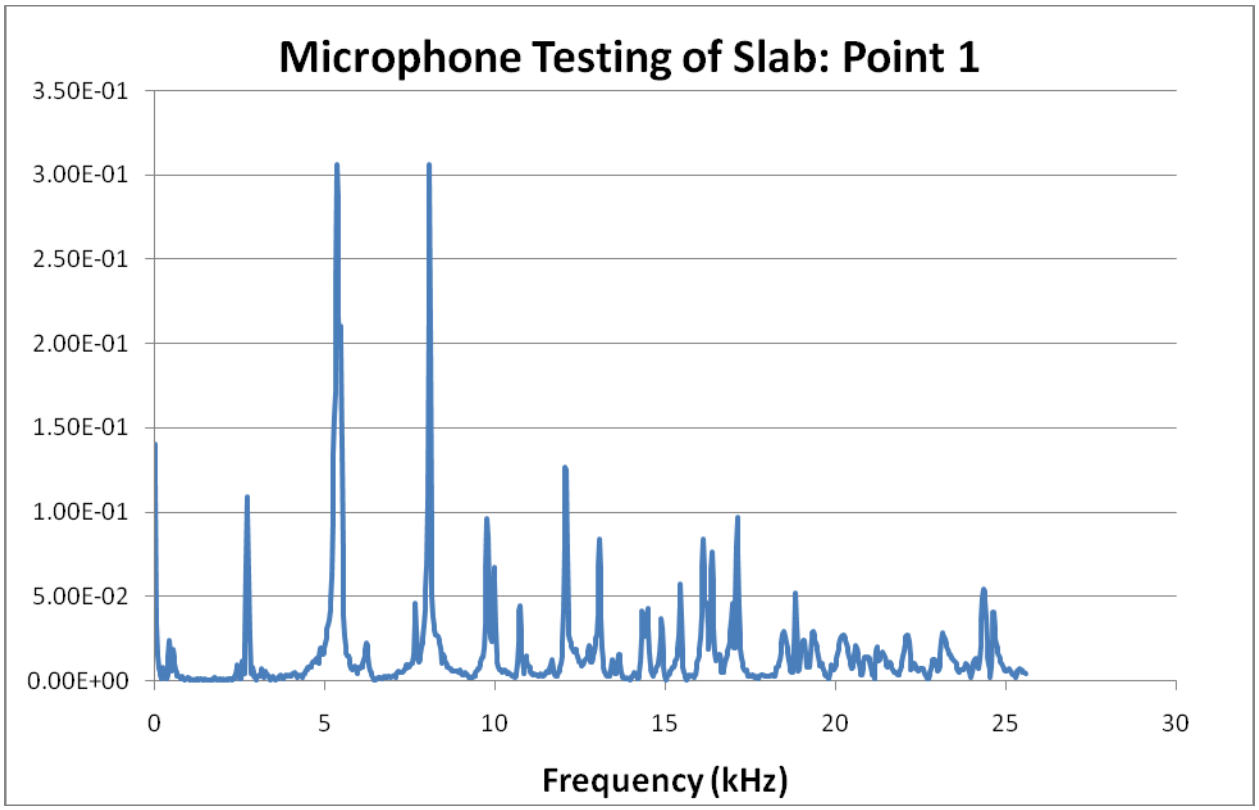

Figure 19: Air-coupled impact-echo results for point 1 (shallow defect).

As a result of the laboratory testing, the following recommendations were made for further testing, including laboratory and field studies that followed this testing program.

- Locate the depth of the reinforcement by testing generally in the proposed testing region to find a consistent, deep signal.
- Watch for shifts in the first mode frequency and consider them a better indicator of the presence of small defects near the surface than the higher modes frequencies.
- Look for deviations from the general pattern determined, especially at higher frequencies to locate deeper defects.

Modal Analysis Results: Beams

The FRF of testing seven points along the length of the beam was obtained from accelerometer and impact hammer records. The combined results were analyzed within the ModalView software by the LSCE (Least squares complex exponential) method. This method produced a user selected sequence of ten frequencies and associated mode shapes for the experiments conducted on the beams. The first four mode shapes were determined to be significant. The analysis of the modal tests of the beams revealed the vibration frequencies shown in Table 5, and the mode shapes shown in Figure 20

Table 5: Observed natural frequencies of trial beams

Mode	Reference Frequency	Rock Pocket Frequency	Foam Insert Frequency
1	64.4 Hz	69.7 Hz	69.0 Hz
2	242 Hz	250 Hz	248 Hz
3	322 Hz	380 Hz	348 Hz
4	393 Hz	435 Hz	397 Hz

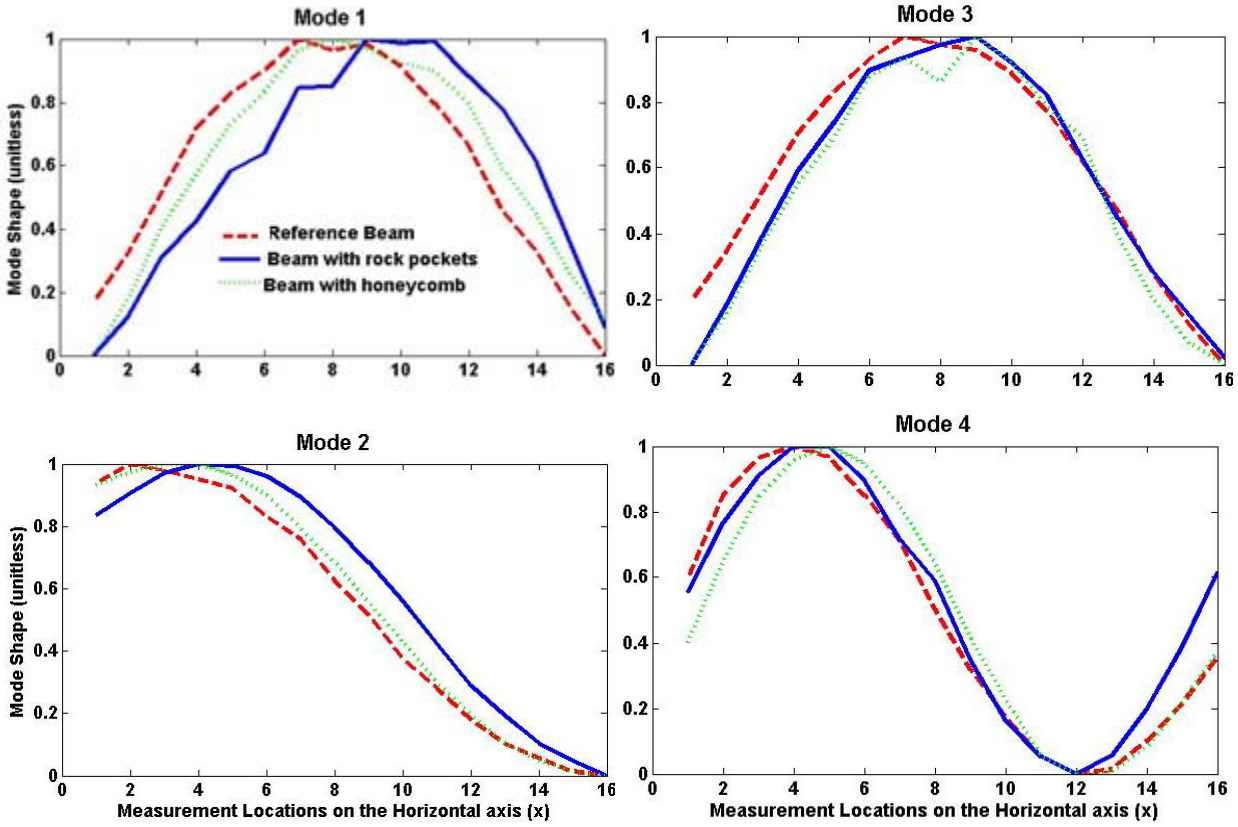

Figure 20: Laboratory-observed mode shapes of trial beams.

Findings of Field Testing Program

IEI Impact Echo

The testing program on the slab/joist system in Room 221 of Building 18F was able to detect the differences in thickness between the slab and the joists and to provide a good estimate of the thickness of each of these components, even without access to the bottom of the slab.

The cross section of the slab joint system is shown in Figure 21 below. Figures 22-24 show data from testing of an approximately 4" thick slab and the adjacent joists, with an overall dimension of approximately 8" × 24".

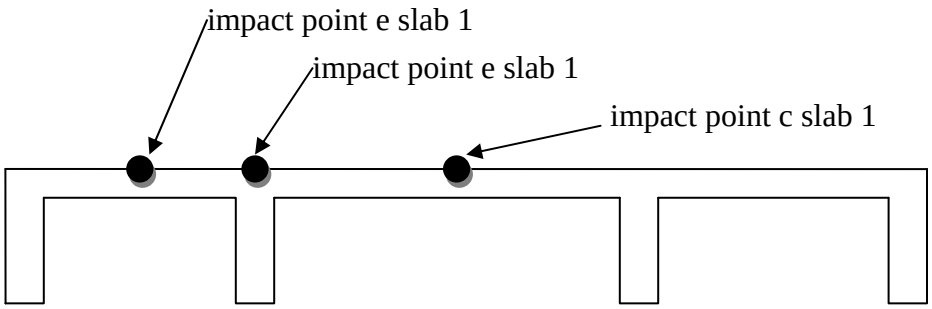

Figure 21: Slab cross-section, Building 18F.

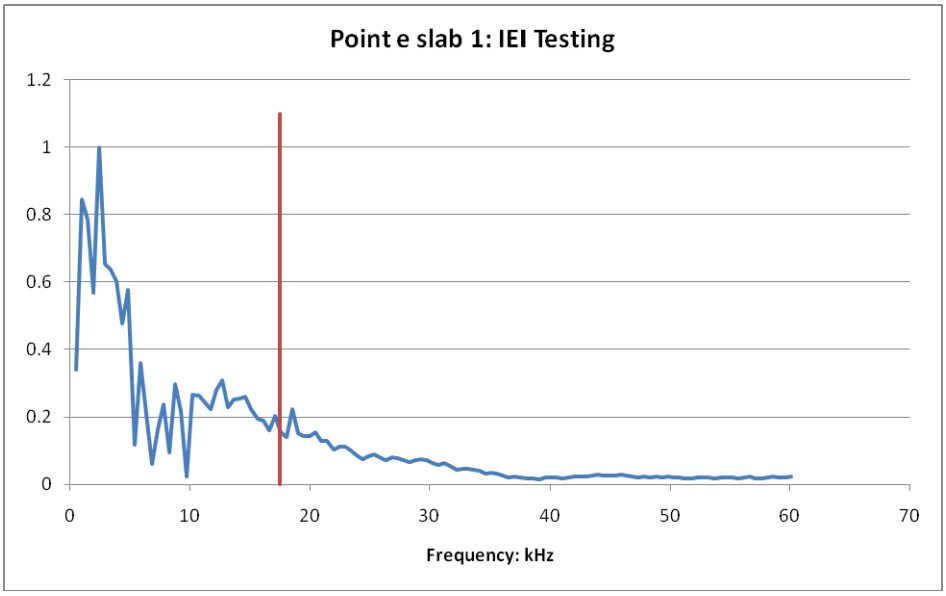

Figure 22: Point E Slab 1, Building 18F, Impact-echo testing using IEI Equipment.

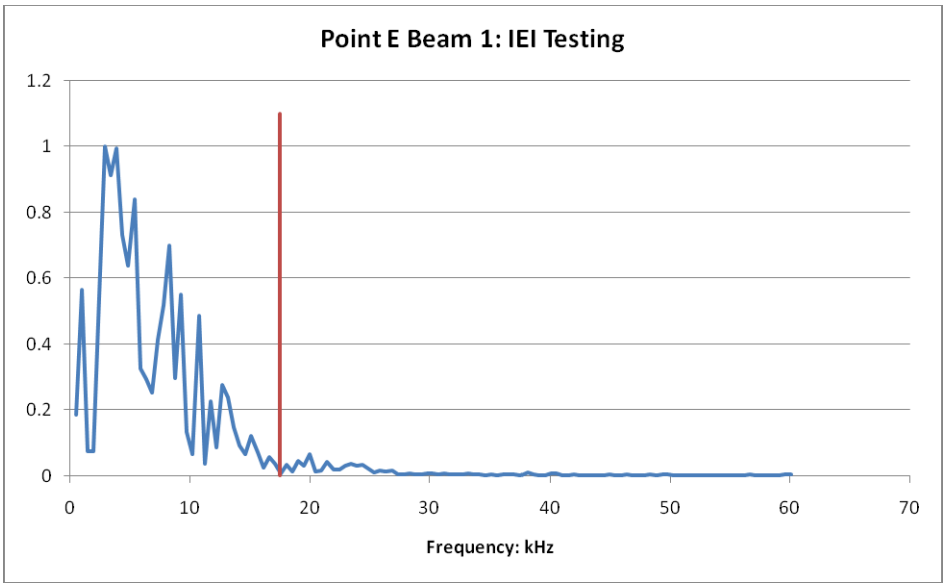

Figure 23: Point E Beam 1, Building 18F, Impact-echo testing using IEI Equipment.

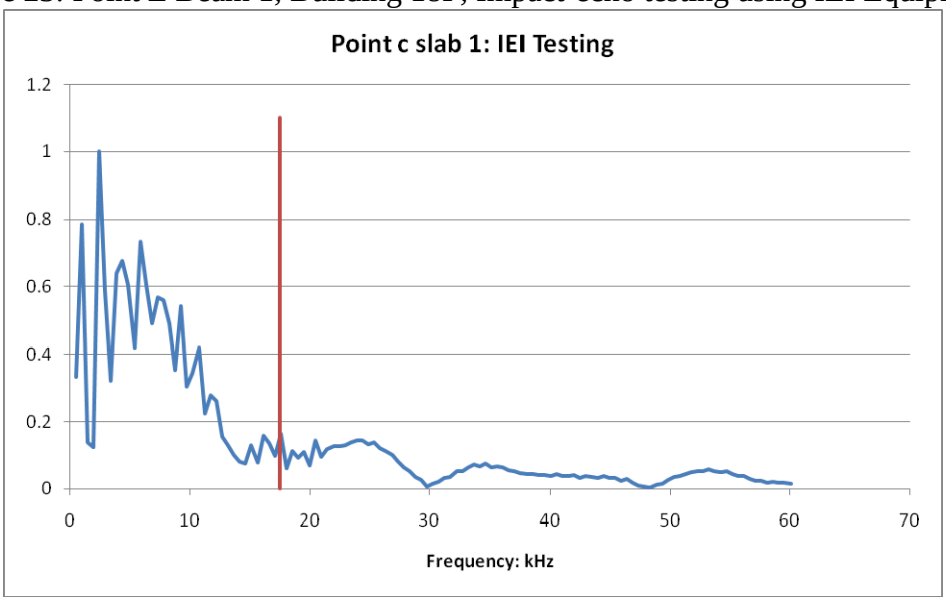

Figure 24: Point C Slab 1, Building 18F, Impact-echo testing using IEI Equipment.

The red line indicates the thickness frequency of the slab. There is a definite response at this frequency, however, the signal is somewhat obscured by lower frequencies resulting from alternative sound paths. The influence of the lower frequencies is slightly greater directly over the beam and it is possible to observe the lower mode frequencies of the sound paths into the beam in the results from point E beam 1. These signals would be difficult to distinguish without prior knowledge that they are taken in a slab away from a beam and at the beam, but the content of the signals is consistent with what is known about the impact-echo response of slabs and beams.

The testing program conducted on the pedestals in Building 19 showed the utility of this type of testing. A through-thickness frequency spectrum is taken from a test on a normal area of a 12"× 24" pedestal. The spectrum (Figure 25) shows a thickness frequency at the anticipated level of

5.1 kHz and very few higher-frequency return signals, indicating very little disruption of the sound wave through the thickness of the pedestal. If there were a reinforcing layer at the far side of the pedestal, it would show as a larger signal at a slightly higher frequency. Most tests on the pedestals in Building 19 did not show the presence of reinforcement. A spectrum (Figure 26) taken on the same pedestal in the region of a small, but apparent, crack shows the disruption in the pattern of frequencies caused by the internal crack. The additional peaks at 10 and 15 kHz indicate that sound waves are being reflected by an internal obstruction, such as a crack or an inclusion, at approximately one half (10 kHz) and one third (15 kHz) of the thickness of the pedestal. Illustrations of typical patterns of damage in the pedestals are shown in Figures 27 and 28.

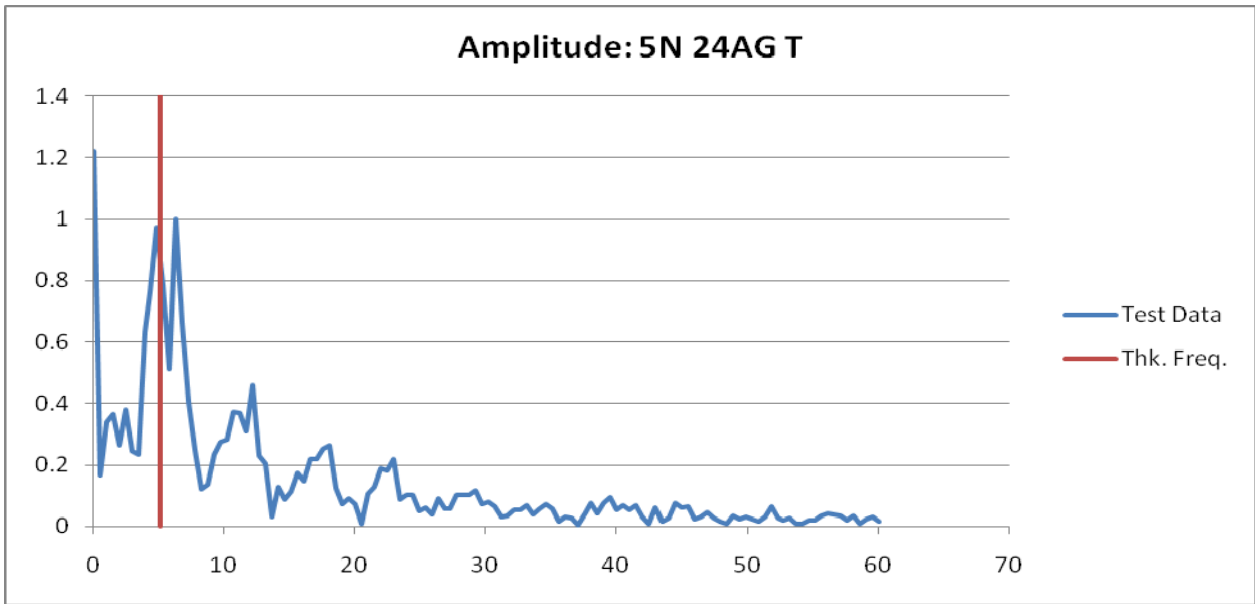

Figure 25: Impact echo plot, pedestal 5 north, 24" above ground, transverse.

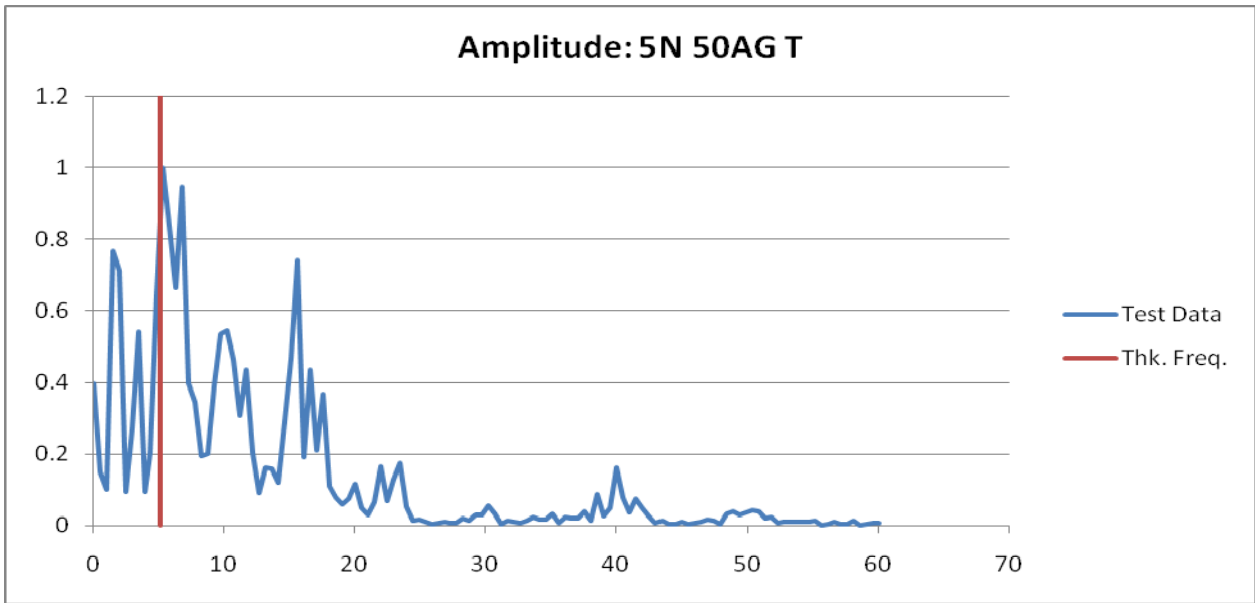

Figure 26: Impact-echo plot, pedestal 5 north, 50" above ground, transverse.

Figure 27: Pedestal 5 north: largely intact, with diagonal crack at 50".

Figure 28: Pedestal 1 north: severely damaged pedestal.

Air-Coupled Impact Echo

Floor of Building 18F

A series of experiments was run on grid points laid out in the floor of Building 18F, using the air-coupled impact-echo system. Results are shown for the points E Slab 1, E Slab 3, and E Beam 1, representative of the slab and the beam results obtained (Figures 29-31). The expected fundamental frequency of the full depth of a joist is 2.8 kHz, and the expected thickness frequency of the slab is 11.5 kHz.

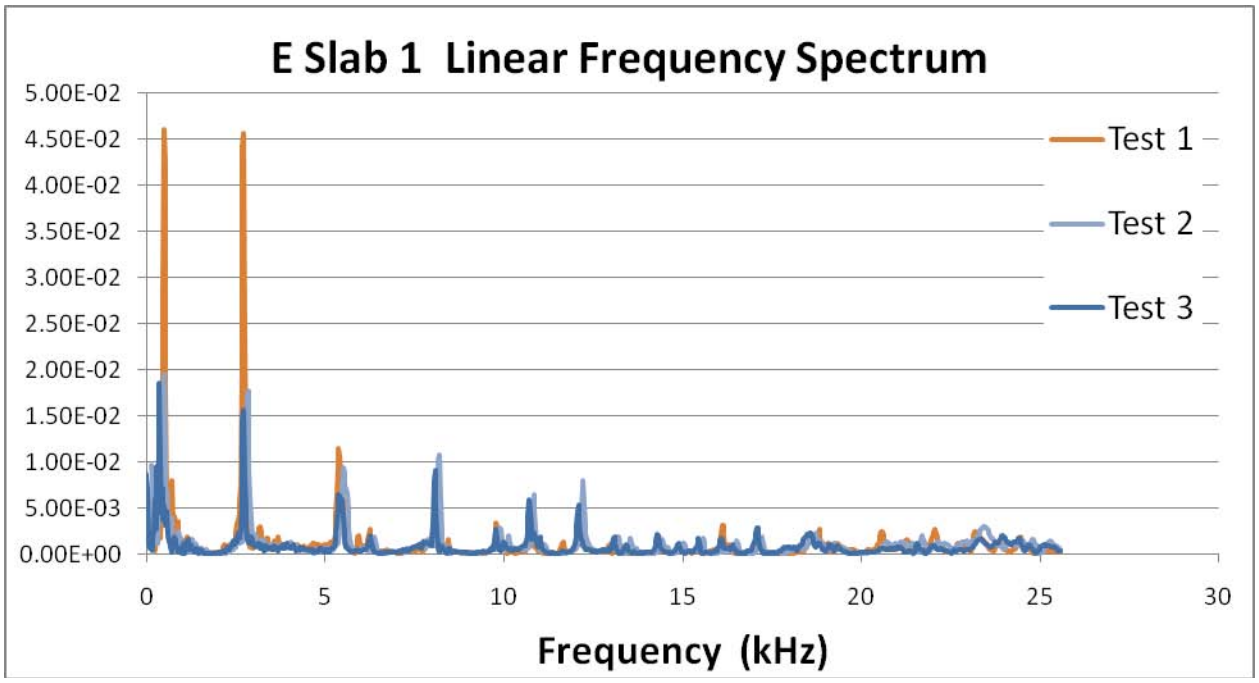

Figure 29: Point E Slab 1: Impact-echo testing using air-coupled method.

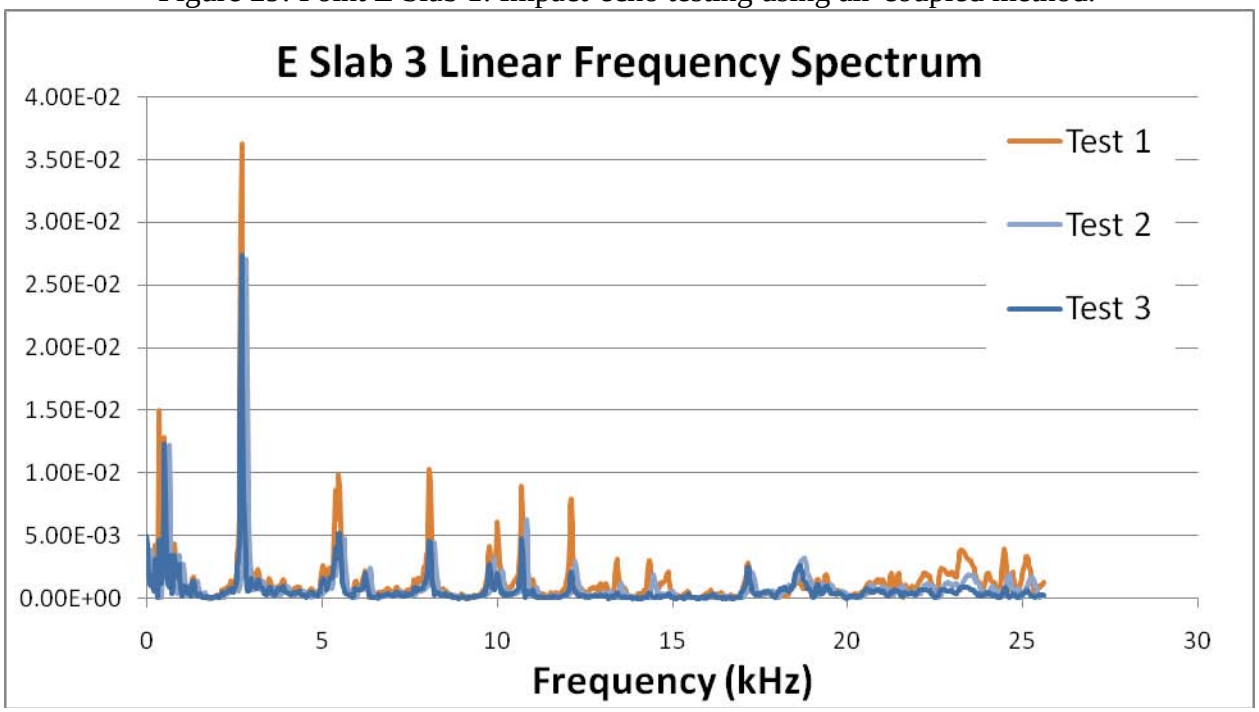

Figure 30: Point E Slab 3: Impact-echo testing using air-coupled method.

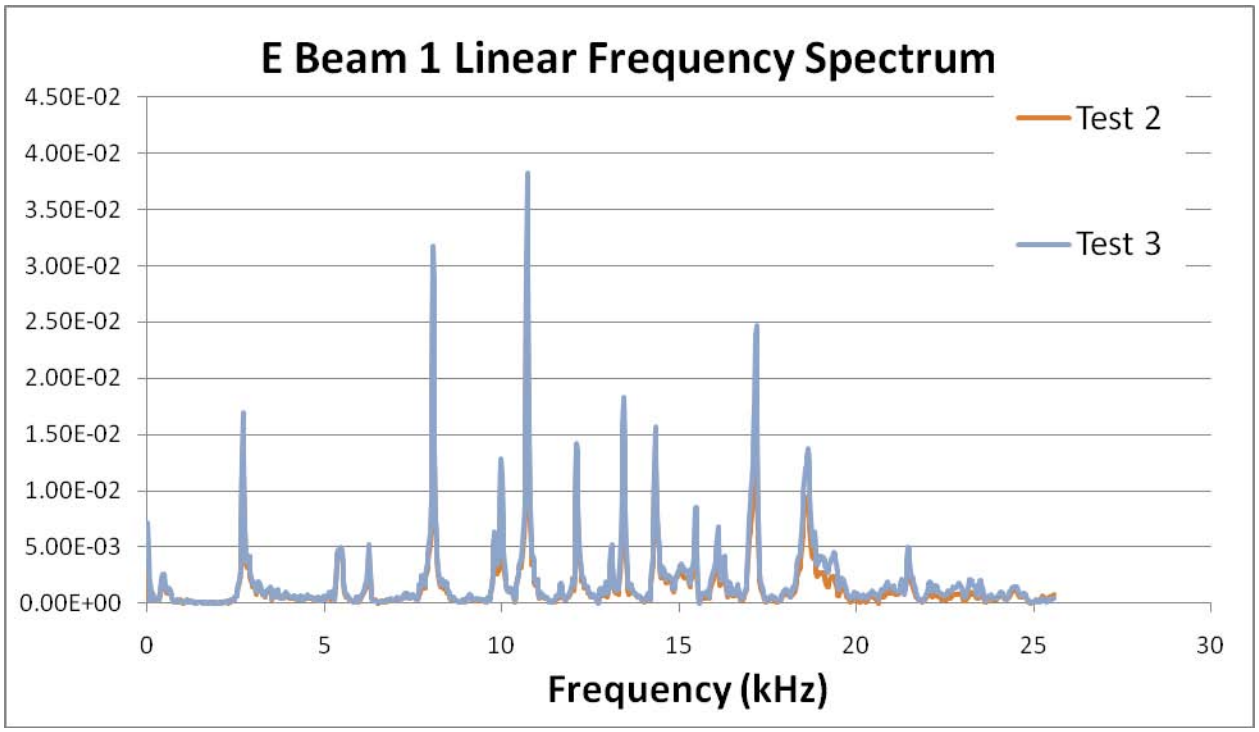

Figure 31: Point E Beam 1: Impact-echo testing using air-coupled method.

An alternative diagonal path to the corners of the joist-slab interface has an expected frequency of approximately 9.7 kHz.

The results from the air-coupled impact-echo show a larger amount of data than the results of the IEI system. A significantly greater number of peaks are observable, and they are more easily distinguished. In particular, the fundamental frequency of the beam is discernable in each of the plots. The frequency of the slab virtually vanishes from the beam test, but is noticeable in the slab tests. The difference in character between the beam test and the slab tests is also very noticeable, in that a large number of intermediate frequencies between the beam and the slab mode are noticeable. These frequencies correspond to the higher modes of response of the beam. A review of the data taken throughout the floor slab grid indicates that the slab-joist system is fundamentally sound. No evidence of significant internal cracks or defects was observed during the testing program on this slab.

Column Test: A typical set of test results on a 24" square column is shown in Figure 32. These tests were all conducted on the same column, at the same location 12 feet above the floor, using the air-coupled method.

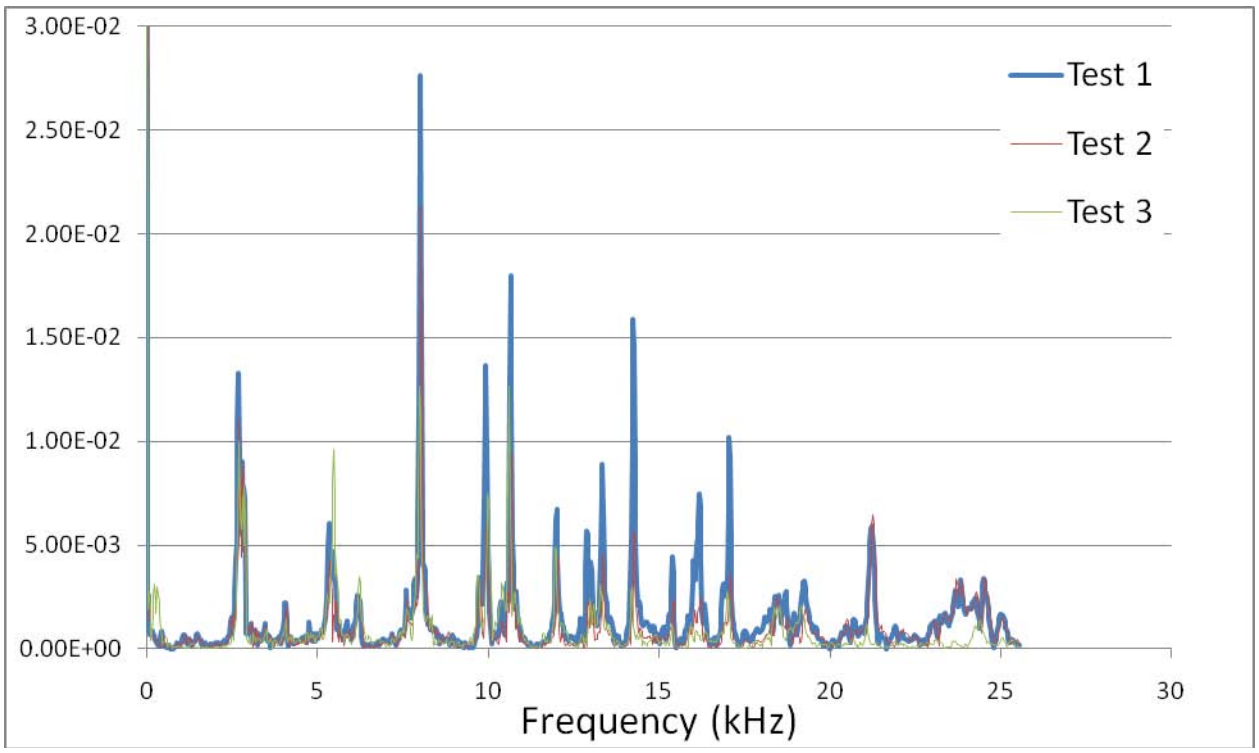

Figure 32: Air-coupled impact-echo result on a column: Building 18F.

The following are the expected thickness frequency and the first three higher modes, using a p-wave velocity of 3500 m/s

Thickness frequency	2.5 kHz
Mode 1	3.6 kHz
Mode 2	4.8 kHz
Mode 3	4.9 kHz

These frequencies are slightly offset, with strong peaks at 2.7 kHz and 5.4 kHz, and a weak peak at 4.1 kHz. This indicates that the p-wave velocity in the concrete of the column is approximately 10-12% greater than that estimated, that is approximately 3800 m/s. This indicates a probable concrete modulus of elasticity of 33,000 N/mm^2, hence a strength of approximately 49 N/mm^2 (7000 psi). This is partially substantiated by tests using a Schmidt rebound hammer, for which an estimated strength of >6000 psi (upper limit of the conversion scale) was recorded.

Floor of Building 18F in combination with partially automated impact system.

Accelerometers were located in the center of the floor of Building 18F (Points 11 and 13) during the testing of the automated impact system. Although the impacts of the air-driven balls were low-energy compared to the effect of the impact hammer generally used in experimental modal analysis, the response of the accelerometers was sufficient to trigger the system and allowed a waveform to be recorded. A series of frequency response functions, for use in modal analysis, could be constructed using the input of the impact and the response of the accelerometers. This

procedure was attempted for the impact of a 5/8" diameter ball, and the resulting frequency response function was more characteristic of a through-slab response, such as in the impact-echo method, than a global response of the slab, as required for experimental modal analysis.

Pedestals of Building 19

As described previously under impact-echo testing, the piers showed several patterns of cracking, including diagonal cracks near the base. The two charts below show a comparison of the impact-echo results for pedestal 6N (Figure 33), which was visibly intact, and pedestal 8N, which had significant cracking near the base (Figure 34).

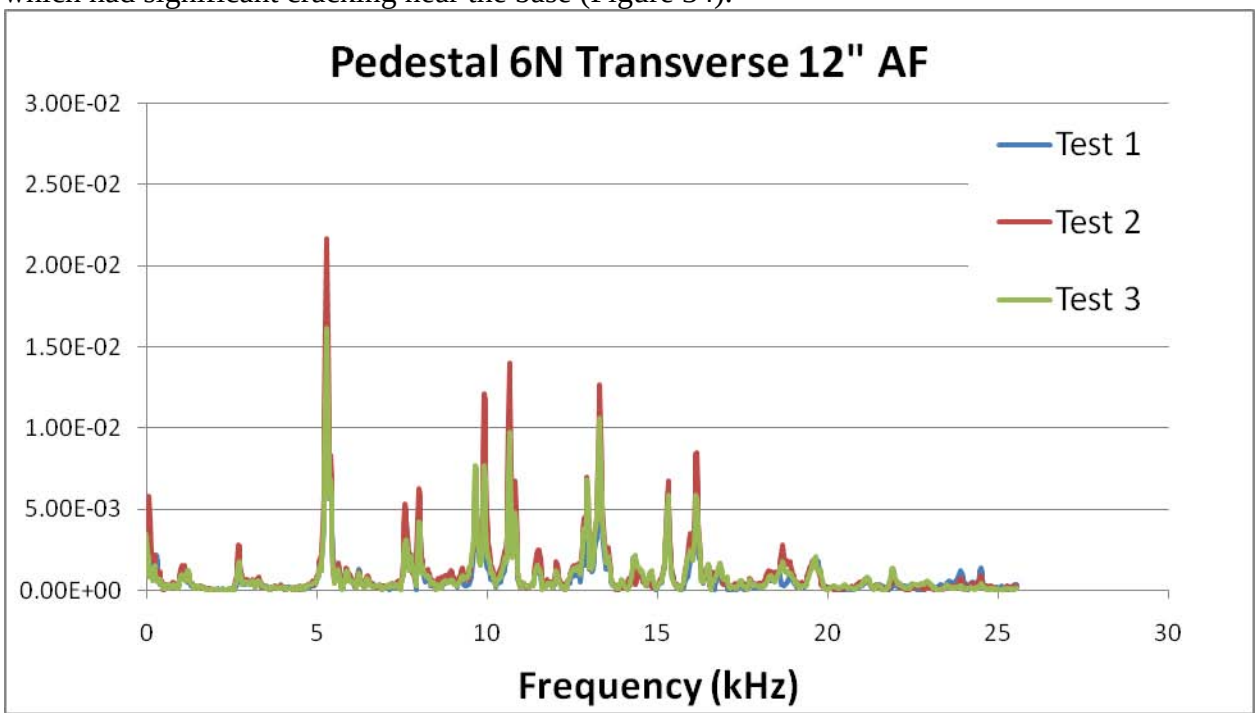

Figure 33: Pedestal 6N Air-coupled impact-echo result.

In the plot from pedestal 8N, the damage is evident in several features of the frequency spectrum. The fundamental period of 5.3 kHz is much attenuated, indicating that few of the p-waves generated by the impact were able to penetrate to the opposite face of the pier. The presence and importance of a large number of higher frequencies is also a general indication of damage. Finally, the double peaks that are observable in the plot from pedestal 8N appear to be a further indication of damage. These double peaks may result from reflections off the two faces of a crack.

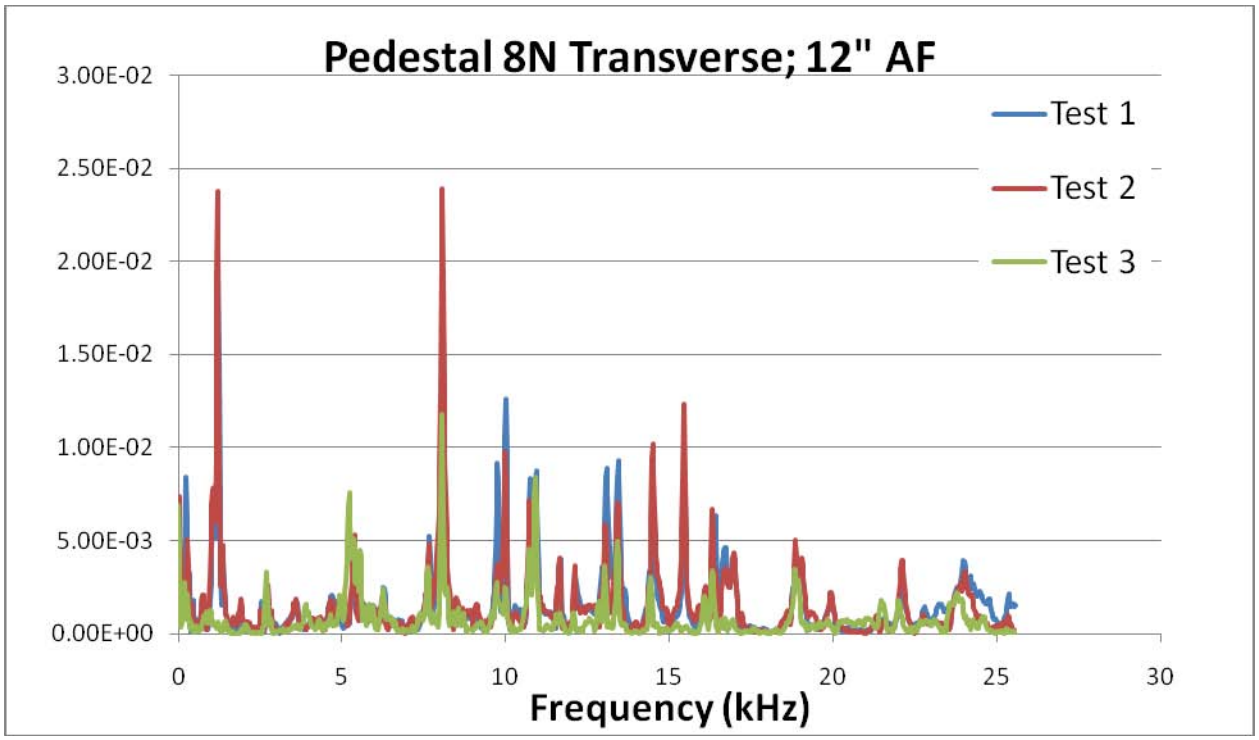

Figure 34: Pedestal 8N Air-coupled impact-echo results.

Walls of Building 19.

The exterior walls of Building 19 were tested in accordance with the procedure described in the Materials and Methods section of this report. An example of a record taken on a substantially intact segment of wall is shown in Figure 35 below. Based on considerations discussed later, the p-wave velocity in the bricks in this wall is found to be approximately 2000 m/s, resulting in a thickness frequency for the full 0.40 m thickness of the wall of 5.0 kHz. From this, the depth of other signals can be inferred, as shown on the figure below. Since point 7.3N2 is on a stretcher, the signal for the full thickness frequency is relatively low amplitude. A very large peak is visible at approximately the joint between the two wythes of brickwork, and a few additional disturbances at higher frequencies indicate the presence of defects closer to the surface.

The data in the Figure 36 was taken at a lower level partially on a header and partially on a stretcher (the lower row of tape marks can be seen in the photograph). They show a complicated superposition of signals from the two areas of wall, and the additional presence of a significant level of defects in the wall. The peak around 5 kHz for the full thickness of the wall is larger because of the presence of the header. Given the 20 cm thickness of the wall, this allows the p-wave velocity to be calculated at approximately 2000 m/s.

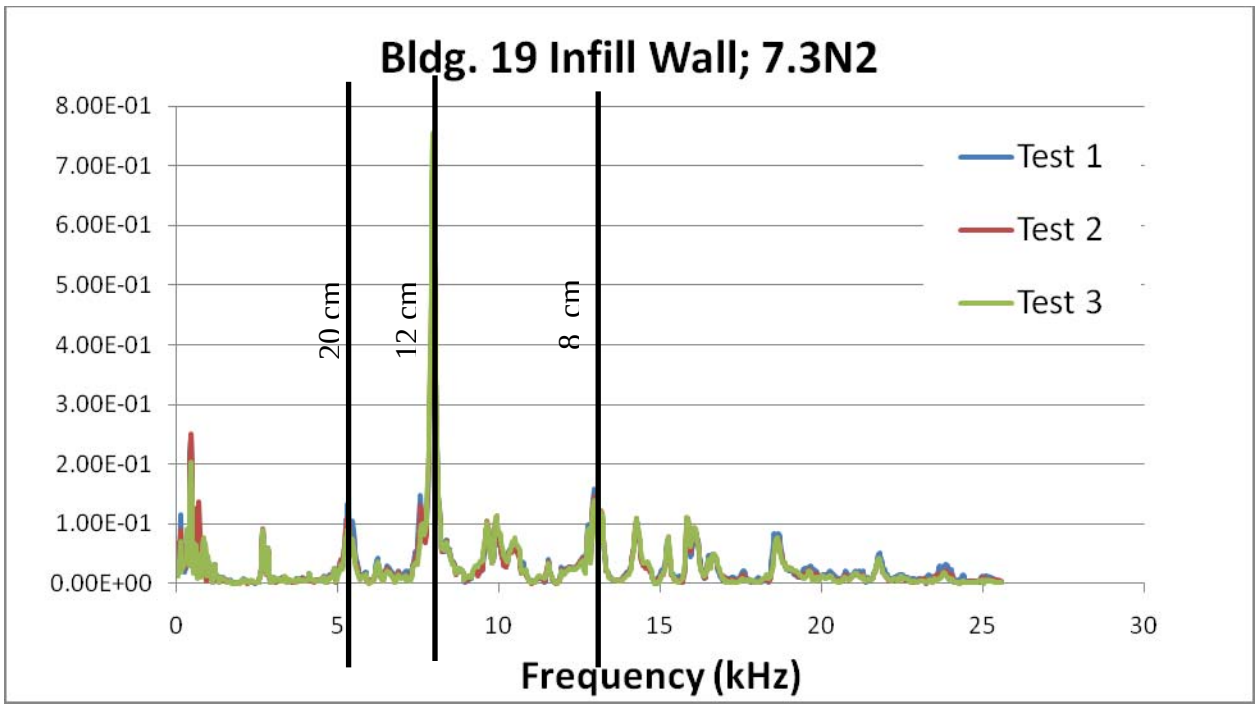

Figure 35: Air-coupled impact-echo results of intact two-wythe masonry: Building 19.

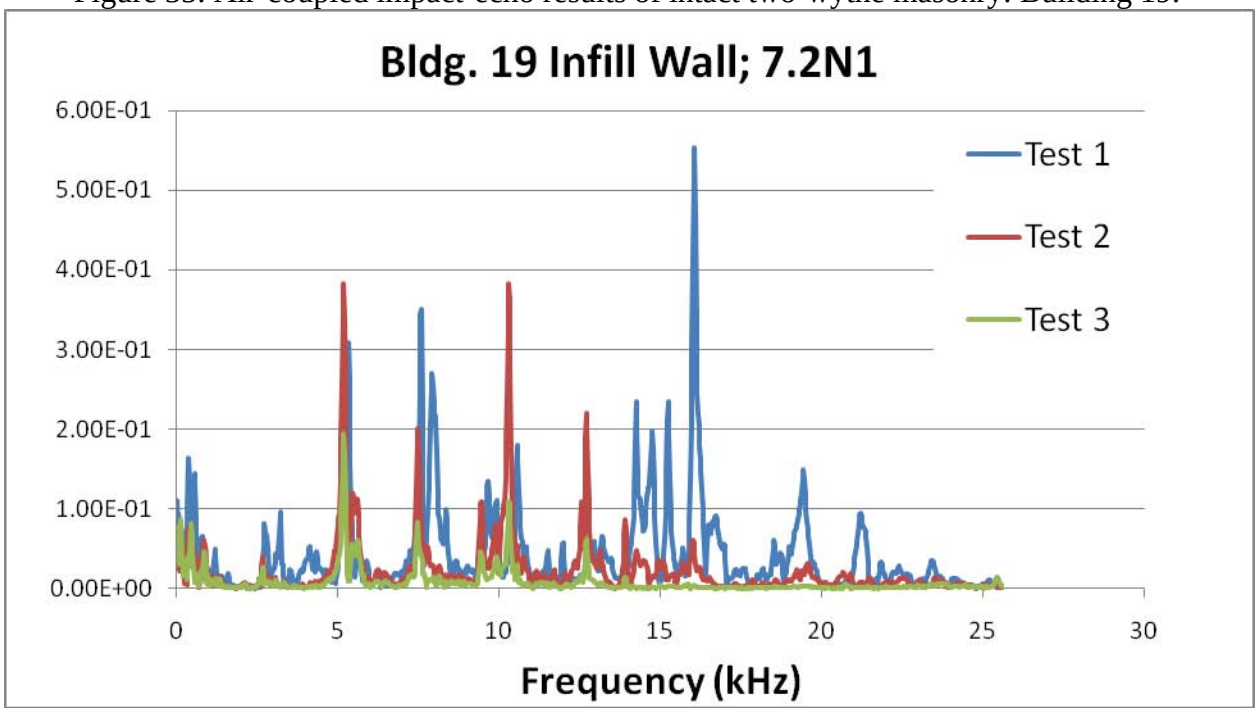

Figure 36: Air-coupled impact-echo results of header course of masonry wall: Building 19.

Figure 37 shows a section of wall adjacent to the lintel bearing that has sustained a significant level of damage. The widely distributed high frequency peaks, above levels seen for normal brickwork are a clear indication of the damage that the wall has sustained in this location.

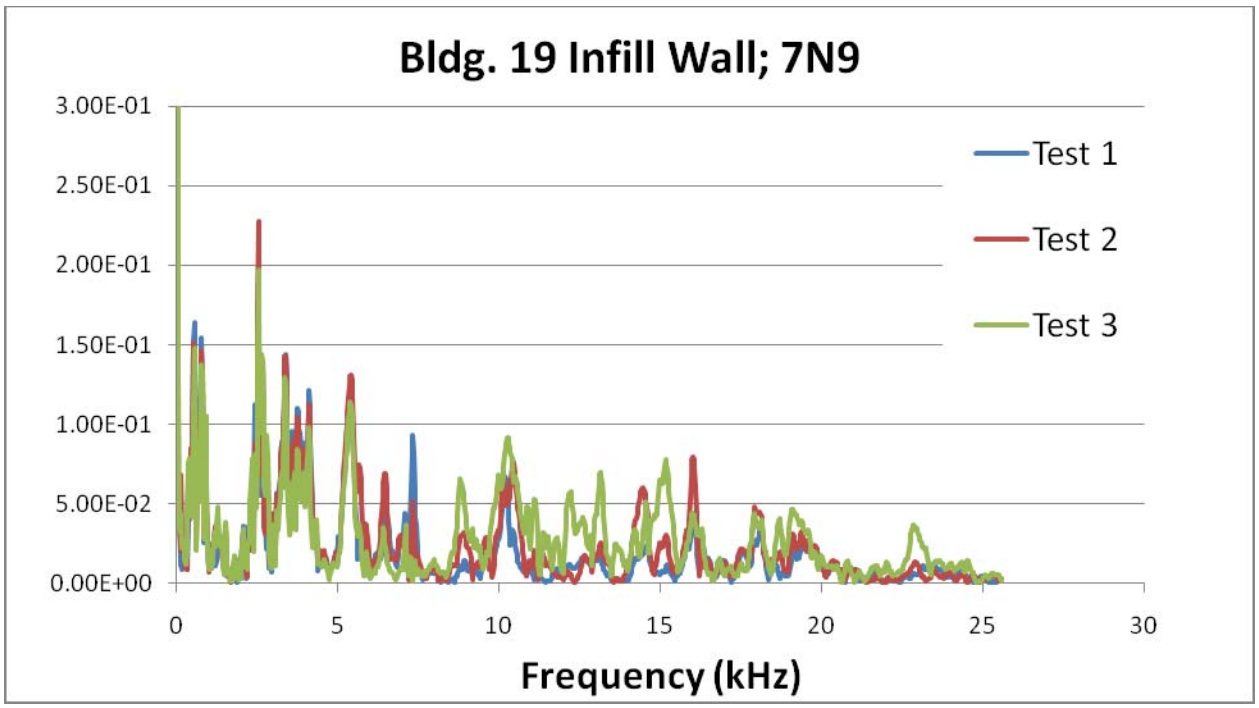

Figure 37: Air-coupled impact-echo results of damaged section of masonry wall, Building 19.

The results of this investigation show that, by taking careful initial baseline measurements, that significant information about a masonry wall can be inferred using the air-coupled impact echo method. This method can be combined with other diagnostic procedures to arrive at a more complete picture of the state of a historic masonry wall.

Modal Testing

The floor in Room 221, Building 18F was subjected to a modal testing program to determine the frequencies and mode shapes of one bay of the floor system. The cross-section of the joist-slab system is shown in Figure 21, while the plan of this bay is shown in Figure 10. The processing of the modal test data resulted in the frequencies shown in Table 6

An image of the first four mode shapes is shown in Figures 38-41. The first mode is a simple single-curvature bending, while the second mode involves primarily slab bending and includes a nodal line at the center joist. The higher modes include increasing involvement of bending of the joists. The character of the lower mode shapes is predictable for an intact system of slabs and beams, implies that the slab system is undamaged. The symmetry of the mode shapes, the lack of bending adjacent to the beams, and the low amplitude of the vibrations are all indicative of the lack of general damage to the structural system.

Table 6: Experimentally-determined mode shapes of floor slab in Building 18F

Mode	Frequency (Hz)	Damping (% of critical)
1	32.7	6.6
2	50.7	7.1
3	91.8	3.7
4	112	4.0
5	145	2.1
6	153	3.2
7	172	4.0
8	182	1.6
9	189	1.1
10	195	1.7

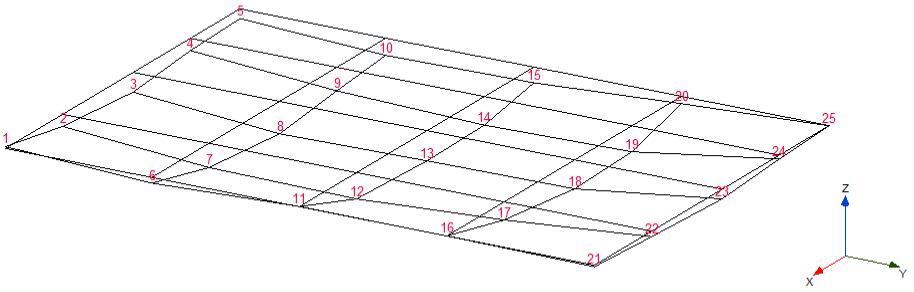

Figure 38: Building 18F slab: mode 1.

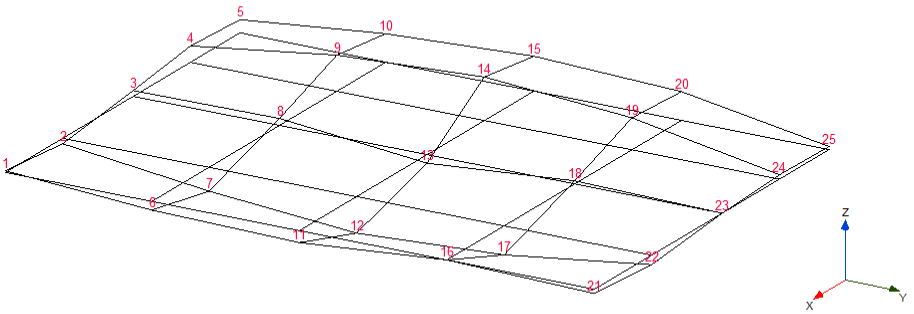

Figure 39: Building 18F slab: mode 2.

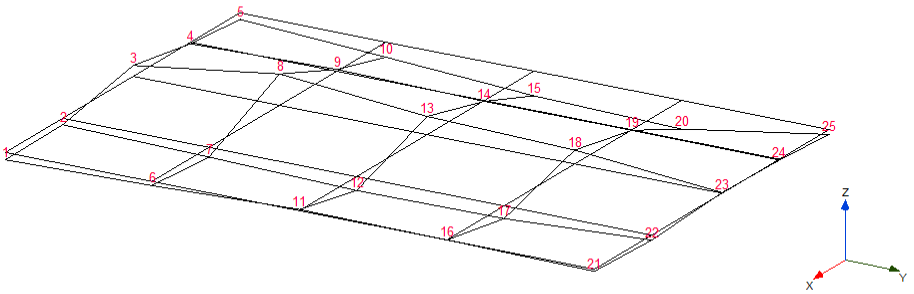

Figure 40: Building 18F slab: mode 3.

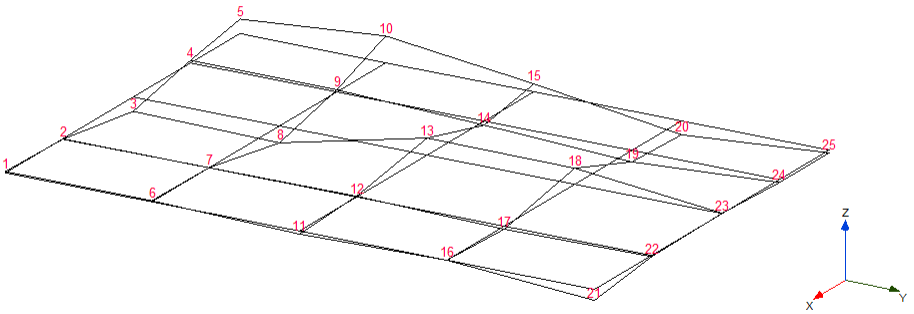

Figure 41: Building 18F slab: mode 4.

Conclusions and Implications for Future Research

Conclusions

The air-coupled impact echo method is a significant and useful means of conducting investigations of historic masonry and concrete structures. The method has to be applied with care and intelligence. The findings of an impact echo survey require that at least a few known undamaged and known damaged areas be surveyed in order to determine the general patterns of the response of the material. Some defects can be more difficult to locate by the method, although the presence of the defects may be apparent. The method will be considerably enhanced by allowing real-time viewing and comparison of data from different locations. The application of this method to masonry structures, both load-bearing and non-load-bearing, can be very effective; however, the heterogeneity of the material may make interpretation of the signals difficult.

This method has been successfully applied to a number of different types of structures at an Air Force installation. A reinforced concrete floor was investigated in detail. It was possible to determine the thickness of the floor slab based on air-coupled impact echo methods, but the absence of defects in the floor made it difficult to comment on the effectiveness of this method in determining defects. The method was also applied to unreinforced concrete pedestals in a building constructed in 1927 (Building 19, Area B, Wright-Patterson AFB). The absence of reinforcement was apparent in the impact-echo results, and the disturbance created by other cracks in the pedestals could also be noted from the frequency spectra produced by this method. The method was also capable of significant findings in the exterior masonry wall of the same building. The thickness of the wall could be determined, headers could be distinguished from stretchers, and the presence of defects could be determined by this method.

Current software makes the experimental modal analysis method significantly easier to apply to a building structure. The method often yields useful information about the overall behavior of the structure with minimal disruption to the structure or its occupants.

This method has also been implemented at Building 18F, Wright-Patterson AFB. A joist-slab-beam system was tested by the EMA method, and the main frequencies and modes of vibration were determined. The response floor slab responded normally, and showed that it had not sustained any obvious form of damage.

Significant progress was made in the development of an automated system for conducting impact-echo studies. The impactor described in this study has been assembled and has been used to propel steel balls to create the dynamic impacts used in impact-echo studies. An early prototype of this system was used in further testing of the floor in Building 18F, Wright Patterson AFB. The software necessary to control the impactor and the data acquisition system has been partially developed. Given the success of the air-coupled impact-echo method, it is apparent that this method can be integrated with the automated impactor and data acquisition. This process is described more fully in the description of the Future Implications of this work.

The current system, as developed, is capable of conducting condition investigations into historic masonry and concrete structures. The air-coupled impact echo system that has been developed under this project can be used very effectively for the characterization of the strength of in-situ concrete and masonry, and for the identification and localization of defects in the building fabric of historic buildings constructed with these materials. The particular form of the impact-echo method adapted for this project allows the operator to move easily from point to point by relocating the microphone enclosure. The system can be further automated for scanning operations by adding positioning software to the data acquisition software. This system can then be used to cover large expanses of floor or wall.

Experimental modal analysis has also been carried out successfully in this project using software compatible with that used for the impact-echo analysis. The coverage of an area by roving the impact, and the processing of the data to identify frequencies and mode shapes has proven relatively simple for a method that is inherently complex. It has further been shown possible to excite the accelerometers for a modal analysis using the same impactor as for the impact-echo analysis, although the bandwidth and energy of the excitation need to be made compatible with this method. It is clear, however, as was done in Building 18F, that it is possible to conduct a complete impact-echo and experimental modal analysis survey in a very limited span of time, and to achieve meaningful results from these surveys.

The integration of impact-echo and experimental modal analysis is certainly possible within the present framework. The software used for the analysis of both sets of results is compatible, because both programs utilize the LabVIEW compiler. The same impact can be used to excite both the microphones used in impact-echo and the accelerometers used in EMA. However, a significant further effort in writing software is necessary to achieve the desired integration of the two methods.

Future Implications

Further development of this system will focus on automation and integration. The programming of the impact-echo system to include: triggering the impacts, locating the impact point on a grid, capturing the data, generating the frequency spectrum, and then post-processing all impact events to render a visual indication of defect locations can be completed with a few months of additional prototyping and experimentation effort. Further development of the impactor to be more portable and reliable and to operate properly at any angle will require an additional year, but will eventually result in a system that is useful on its own. Over a period of two years, we will be able to combine this automated air-coupled impact echo system with a system to complete a modal analysis of a structure, such as a wall or a structural floor slab. In general, such a system would use air-driven steel balls for impact, microphones for impact-echo data acquisition, and a few fixed accelerometer locations to acquire data for modal analysis. The impacts, because they are roving through all the grid points of the structure, can generate enough data to complete a modal analysis, but the required energy and duration of the impact needs to be determined. The eventual addition of this capability will be a significant enhancement to this system.

In addition to further software development efforts to integrate air-coupled impact echo and experimental modal analysis software into a combined software package and to operate the automated impactor apparatus, efforts are also ongoing to improve the utility of the automated impactor system.

In the near future, automated impactor system development efforts will focus on precise calibration of the equipment for pneumatically-propelled steel ball impactors ranging in size from 1/8 in. to 2 in. diameter. Impactor acceleration and impact force curves at various air pressures and barrel-to-impact surface distances for each ball size will be developed using high speed video, custom-built chronograph hardware, and dynamic strain recordings during impact events. Development work is also ongoing to reduce the size and overall weight of the automated impactor system. Initial work is focused on optimizing propellant storage and delivery components. Necessary modifications to the impactor for flexible use of higher pressure propellants is also being considered. Optimization of barrel length and changing the barrel/barrel mount materials of construction from metal to plastic or composite materials can reduce the overall weight of the impactor to allow potential integration of propellant storage and delivery components at the impactor device. Conversion of the impactor system electronic and data acquisition hardware to a microcontroller-based design will also allow integration of the electronic packaging onboard the impactor device. When coupled with an automatic ball loading apparatus also being designed for the system, these enhancements are expected to improve the utility of the system. The improvement of this system will open up the possibility of a wirelessly-operated, totally-automated, scanning system for constrained or remote areas.

In the present study, the concept of using air-coupled impact echo as a method for locating defects in concrete or masonry buildings has been demonstrated. The feasibility of integrating this system with diagnostic investigations by Experimental Modal Analysis has been demonstrated. A prototype of an automated impactor for scanning studies of floor slabs or walls has been constructed. Initial software development to achieve integrated operation of this device has been done. Further effort, outlined in the section above, will be necessary to complete the development of the concepts described in the body of this report. The result of this future effort will be an integrated partially automated scanning system by which a single operator can complete a defect study of a large area of floor or wall of a historic concrete or masonry structure efficiently.

Literature Cited

Atamturktur (2009). *Calibration under uncertainty for finite element models of masonry monuments.* Ph.D. Dissertation, The Pennsylvania State University.

Berriman, J., Hutchins, D., Neild, A., Gan, T., and Purnell, P. (2006). The application of time-frequency analysis to the air-coupled ultrasonic testing of concrete. *IEEE transaction on ultrasonic, ferroelectrics and frequency control*, 53(4):768-776, April.

Choubane,B., Fernando,E., Ross,S.C., Dietrich,B.T. (2003). Use of ground penetrating radar for asphalt thickness determination. *Proceedings of the SPIE - The International Society for Optical Engineering*, 5045:230-40.

Sansalone,M., and Carino,N.J. (1989). Detecting delaminations in concrete slabs with and without overlays using the impact-echo method. *ACI Materials Journal*, 86(2):175-184, March.

Sansalone, M., and Streett, W. (1997). *Impact-echo: nondestructive evaluation for concrete and masonry*. Bullbrier Press, Ithaca, 336pp.

Zhu, J (2005). *Non-contact NDT of concrete structures using air-coupled sensors*. Ph.D. dissertation, Univ. of Illinois at Urbana-Champaign, Urbana Ill.

Zhu, J., and Popovics, S. (2002). "Non-contact detection of surface waves in concrete using an air-coupled sensor," *Review of progress in quantitative nondestructive evaluation*, D.O. Thompson, and D.E. Chimenti, eds., American Institute of Physics, Melville, N.Y., pp. 1261-1268.

Zhu, J., and Popovics, S. (2007). Imaging concrete structures using air-coupled impact-echo. *Journal of Engineering Mechanics*, 133(6):628-640, June.

ASTM (American Society for Testing and Materials) Standards Referenced in this Report

ASTM C 42. *Standard Test Method for Obtaining and Testing Drilled Cores and Sawed Beams of Concrete*. American Society for Testing and Materials, Conshohocken, PA, 2004.

ASTM C 1196. *Standard Test Method for In Situ Compressive Stress Within Solid Unit Masonry Estimated Using Flatjack Measurements.* American Society for Testing and Materials, Conshohocken, PA, 2009.

ASTM C 1997. *Standard Test Method for In Situ Measurements of Masonry Deformability Properties Using the Flatjack Method.* American Society for Testing and Materials, Conshohocken, PA, 2009.

ASTM C 1314. *Standard Test Method for Compressive Strength of Masonry Prisms.* American Society for Testing and Materials, Conshohocken, PA, 2010.

ASTM C 1587. *Standard Practice for Preparation of Field-Removed Manufactured Masonry Units and Masonry Specimens for Testing.* American Society for Testing and Materials, Conshohocken, PA, 2009.